ATOM DENSITY MEASUREMENTS BY LUMINESCENCE OF SOLIDS

By K. M. Sancier, D. J. Schott, and H. Wise

Prepared under Contract No. NASr-49(09) by
STANFORD RESEARCH INSTITUTE
Menlo Park, California

NATIONAL AERONAUTICS AND SPACE ADMINISTRATION

For sale by the Office of Technical Services, Department of Commerce,
Washington, D.C. 20230 -- Price $2.00

CONTENTS

ILLUSTRATIONS

INTRODUCTION

The objective of the present study was to fulfill a current requirement for measurement of oxygen and nitrogen atom densities in the upper atmosphere. Oxygen and nitrogen atom densities at altitudes of 50 to 100 kilometers are of special interest, and in the present work atom densities and pressures anticipated for this range[1-4] were considered.

In this research the experimental basis for atom density measurements is the luminescence produced in solid lumophors by heterogeneous surface recombination of atoms. The luminescence of calcium oxide lumophors excited by nitrogen atom recombination has been described in terms of probable mechanisms of energy transfer.[5-8] These earlier studies provided the background for the present quantitative measurements of oxygen and nitrogen atom densities.

SUMMARY AND CONCLUSIONS

Various lumophors were surveyed in order to find ones suitable for quantitative analysis of oxygen and nitrogen atom densities. Oxygen and nitrogen atoms can best be differentiated by the luminescence intensity: Only CaO lumophors exhibited appreciable response to oxygen atoms, whereas CaO and several other lumophors exhibited appreciable response to nitrogen atoms.

The lumophor CaO:Sb:Cl was selected for a detailed study of oxygen and nitrogen atom densities. The study included an evaluation of (1) the quantitative relationship between luminescence intensity and the atom density measured by electron spin resonance (ESR), (2) the effect of extended exposure to atoms, and (3) the mechanisms of energy transfer leading to luminescence.

The luminescence response of CaO:Sb:Cl to nitrogen atoms was essentially constant upon extended exposure; its response to oxygen atoms, however, showed an exponential decrease with time. For optimum

sensitivity to oxygen atoms and minimum decrease of response, the lumophor temperature should be 400° to 500°K.

The luminescence intensity of the lumophor is proportional to the atom density within certain limits of total pressure and atom density. The departure from a linear dependence for both oxygen and nitrogen atoms is possibly due to excited species produced by the electrodeless discharge.

Atom densities were calculated from ESR measurements using molecular oxygen as a standard of spin density. Confidence in the method derives from the results that (1) the detectability is the same for oxygen and nitrogen atoms (as may be expected for ESR lines of the same line width), and (2) the experimental minimum detectability for these atomic species agrees with the expected theoretical limit of detection by ESR.

With the present equipment the minimum detectable atom density by luminescence of CaO:Sb:Cl is about 1×10^{12} atoms/cc for both oxygen and nitrogen atoms. It is considered feasible to enhance the sensitivity of atom density detection by a factor of 10^5 by refinement of the equipment, on the assumption that the kinetics of the process leading to luminescence remains unchanged at such low atom densities.

The mechanism of the luminescence of solids by surface recombination of atoms and the mechanism by which the luminescence response is decreased because of extended exposure to oxygen atoms are discussed in terms of the solid state properties of catalytic surfaces.

EXPERIMENTAL DETAILS

Many of the experimental techniques employed in this study have been described earlier,[5-8] and for these only brief mention will be made in this report.

Preparation of CaO lumophors was described in detail in reference 6, and the number in parenthesis following a given calcium oxide lumophor refers to the composition given in that reference. The lumophor CaO:Sb:Cl(#3) used predominantly in our experimental work had the following composition:

0.000446 mole fraction Sb, added originally as the oxide (Johnson, Mathey and Co., Limited, "Specpure" grade), and 0.0540 mole fraction KCl added as flux (Mallinkrodt, reagent grade). All the other lumophors studied were of luminescent grade (Sylvania) except CdO and BaO which were of reagent grade (Mallinkrodt). Prior to atom luminescence measurements a lumophor was evacuated and then slowly heated in situ up to 700°K to remove adsorbed gases and water, and then heated at 800°K for 10 minutes (baking process). The oxygen (research grade) and nitrogen (pre-purified) used in the various studies were obtained from the Matheson Co.

The apparatus shown in Fig. 1 was used to measure atom recombination coefficients, heat-generation rates, and luminescence intensities. The basic apparatus is identical to that described in reference 7. For determining atom recombination coefficients the apparatus permits mechanical movement of the lumophor sample so that the lumophor's position with respect to the source of atoms can be changed. The apparatus also provides identical movement of the photomultiplier tube (RCA 6217); hence the lumophor-photomultiplier distance remains constant. An X-Y recorder (Moseley, Model 3S) was used to record the luminescence intensity as a function of distance between the lumophor and the atom source. The signal from the photomultiplier circuit was connected to the Y axis; a helipot, mechanically linked to the rack and pinion (Fig. 1), was used as a potential divider across a battery, and the location of the lumophor was indicated by the voltage output of the helipot which was applied to the X axis of the recorder. When the apparatus was used to measure the heat generated in the solid by atom recombination on the lumophor, a calorimeter was inserted under the lumophor cup in the position otherwise occupied by the heater used to control the lumophor temperature. The heat input was evaluated in the usual way from the slopes of the steady state heating and cooling curves in the presence and absence of atoms. Measurements of luminescence intensity as a function of time and temperature were made in the apparatus shown in Fig. 1 and also in the apparatus to be discussed in connection with Fig. 2. For this work the photomultiplier output was recorded on a strip recorder (Brown). The temperature of the lumophor

could be controlled in the range of 300 to 800°K by the electrical heater in contact with the bottom of the cup which contained the lumophor. The oxygen or nitrogen was dissociated by an 18 Mc radio frequency transmitter capable of dissipating 500 watts in the plate of the output tube. In all studies of luminescence by atom excitation the gases were dried by traps cooled in liquid nitrogen. It was necessary to maintain a constant level of liquid nitrogen; otherwise, whatever material collected in the traps during an extended run (> 30 min) tended to enhance luminescence. This material has not been identified.

The apparatus shown in Fig. 2 was used for measurement of photoexcitation and emission spectra of a variety of lumophors. This apparatus was used in conjunction with that of Fig. 1, and with the same photomultiplier. Two grating monochromators (Farrand) were employed, one to provide light for photoexcitation and the other to analyze the luminescence due either to photoexcitation or atom excitation. An optical "tee" was used to focus the light. It consisted of three quartz lenses and a half-aluminized quartz mirror. The window of the vacuum system also was made of quartz. Excitation or luminescence spectra were recorded directly on an X-Y recorder. The wavelength issuing from a given monochromator was plotted on the X axis of the recorder using a potential derived from a helipot geared to that monochromator. The corrected spectral intensity was plotted on the Y axis. The slit width of the emission monochromator was 200A, of the excitation monochromator 50A. An electronic function generator was used to correct for the spectral response of the photomultiplier and the spectral transmission of the optics. The design of the function generator and the method by which spectral corrections were obtained by its use are described in Appendix A. Photoexcitation and photoemission spectra were measured in a conventional manner; the function generator was not used in these measurements. A 150W xenon high pressure arc was focused by a quartz lens on the entrance slit of the excitation monochromator. To reduce scattered and second-order light, appropriate glass filters (Corning) were placed before the slit of the excitation monochromator and before the photomultiplier.

Simultaneous measurements of atom density and luminescence intensity were made in the apparatus diagramed in Fig. 3. The five main functional parts of the apparatus are the vacuum system, radio frequency discharge, lumophor and heater, optical system, and electron spin resonance (ESR) equipment. The vacuum system consisted of the pumping and pressure-monitoring equipment and the quartz tube assembly which passed through the ESR cavity and in which the lumophor was contained. Pumping was achieved by a mechanical pump and an oil diffusion pump, and pressures were measured by Pirani and McLeod gages. The pressure of the gas to be dissociated was controlled by a variable leak valve (Granville-Phillips Co., Series 9100). Traps cooled in liquid nitrogen were employed in the vacuum lines to the inlet gas, to the McLeod gages, and to the vacuum pumps. The quartz assembly consisted of an Amersil quartz tube, 10 mm o.d., 7.6 mm i.d., and 60 cm long, fused to a quartz tube 38 mm o.d. This assembly was connected to the vacuum system by an O-ring tapered joint (Asco) on one end and an O-ring vacuum gland on the other. An O-ring tapered cap (Asco) was used to seal the end of the vacuum system through which the lumophor was introduced. The entire quartz assembly could be easily removed.

The gases were dissociated by means of a radio frequency electrodeless discharge inductively coupled to a 600W 14-Mc radio frequency transmitter. The atom concentration was controlled by varying the transmitter's power output which was calculated from the product of plate voltage and plate current of the last stage. By adjustment of the vacuum valves (Fig. 3) atom transport from the discharge to the 10 mm o.d. quartz tube could be made to occur either by diffusion alone or by convective flow and diffusion. With convective flow, used for all measurements except recombination coefficients of the quartz, the pressure gradient which occurred along the 10 mm tube was evaluated empirically, and between the cavity and lumophor a distance of 8 cm, it was found to be less than 10%. The oil diffusion pump was used only at total gas pressures less than 55μ. Molecular oxygen was used as a standard of spin density. The pressures referred to subsequently are those in the 10 mm o.d. tube at the cavity, unless otherwise specified.

About 10 mg of powdered lumophor was placed in a small quartz boat (3 mm high and 8 mm long) which was inserted into the 10 mm o.d. quartz tube. The lumophor was heated by a temperature-controlled oven placed during the original assembling of the quartz section, and so positioned that the luminescence of the lumophor could properly pass through the slot in the top of the oven. In all experiments the lumophor was maintained at a temperature at 400°K.

The optical system provided means to focus the luminescence to the photomultiplier (DuMont K 1306), which necessarily had to be mounted well out of the magnetic field of the ESR magnet, and to amplify and record the photovoltage. The focusing was achieved with lens (f/1.2), mirror, and telescoping tubes. The front surface of the photomultiplier was mounted about 60 cm from the center of the magnet, and a shutter was located in the light path to permit correction of any electrical interferences from the magnetic field or radio frequency transmitter. The photomultiplier tube was operated by a regulated power supply, and the output was fed to a microvoltmeter (Kay Lab) where it was amplified and then recorded. It was established that the light from the discharge did not interfere with the luminescence measurements. Because of different geometries and phototubes, luminescence intensities obtained with the apparatus shown in Fig. 3 cannot be considered with those obtained from the apparatus shown in Figs. 1 and 2.

Atom density was measured with a Varian V-4502 X-band spectrometer having a multipurpose cavity (Q of approximately 7000), and employing 100-kc field modulation. The cavity was operated from the low power bridge, and precautions were taken to avoid power saturation. The amplitude of the 100 kc signal to the field modulation coils of the cavity was measured with a peak-peak a.c. voltmeter (Ballantine). A 12-inch magnet (Varian) was mounted on tracks, and the assembly of magnet, bridge, and cavity could be moved to measure atom densities along the 10 mm o.d. quartz tube. The magnetic field was calibrated by a gaussmeter (Bell, Inc., Model 240). The signal to be recorded from the ESR spectrometer was

obtained with the magnetic field adjusted at one of the peaks of the derivative curve of a particular resonance line. The photo and ESR signals were fed to a dual-channel recorder.

RESULTS

A. Comparison of Atom Luminescence and Photoluminescence

Various types of lumophors were surveyed for possible excitation to luminescence by oxygen atoms, by nitrogen atoms, and by photoexcitation. The wavelengths of the luminescence band peaks and their approximate relative intensities were recorded for fresh samples of the lumophors at 300°K exposed separately to nitrogen and oxygen atoms. The photoexcitation and photoemission results were obtained for the lumophors at 300°K. Emission intensities are on relative scales, and the intensity scales of atom and photoluminescence are not related. The results, which are given in Table I, show that CaO lumophors are the most sensitive for detection of oxygen atoms; CaO and several other lumophors were found suitable for nitrogen atom detection.

The atom luminescence spectra of some lumophors excited by oxygen and nitrogen atoms are shown in Fig. 4. The total gas pressure was 16μ and the discharge power 130 watts. For each curve there is a multiplicative factor in parenthesis which indicates the relative scale of the ordinate. The spectra were corrected for the spectral response of the photomultiplier and transmission of the optics (Appendix A).

The CaO lumophor samples used in this study were employed in previous work.[5-8] Some changes in the atom-excited luminescence had occurred. The most pronounced change* was evident for CaO:Mn:Cl(#14) excited by nitrogen atoms for which the 4000A band was now weaker than the 6000A band; also, for CaO:Bi(#7) the 5500A band was now somewhat weaker than the 4000A band.

The CaO:Sb:Cl lumophor exhibits, besides the 4000A band, a weaker luminescence band at about 5500A, presumably due to the Sb activator, which is excited by both oxygen and nitrogen atoms. The intensity of

*These changes suggest that some modification of the solid state properties had occurred since their preparation several years ago.

the 5500A band increases with increase in concentration of the Sb activator, and simultaneously the intensity of the 4000A band decreases. This behavior is much the same as that reported for CaO:Mn lumophors.[6] The intensity of the "activator" band in CaO:Sb:Cl(#3) excited by oxygen atoms is almost undetectable at 300°K, and becomes more intense at higher temperatures.

In order to find suitable lumophors for oxygen atom detection it was necessary to determine, if possible, the reasons some lumophors, and not others, were excited to luminescence by oxygen atoms. Experiments were performed to measure some of the energy transfer parameters involved in atom recombination, and the results are tabulated in Table II. The parameters measured were (1) the atom recombination coefficients, γ'_H and γ'_L as measured from heat and luminescence respectively;[7] (2) the luminescence intensity L; and (3) the rate of heating H of the lumophor due to atom recombination measured from the rate of resistance change (Ω/min) of a thermistor in the calorimeter. Most of these measurements were made for the three lumophors -- CaO:Sb:Cl(#3), CaO(#19), and $MgWO_4$, and separately for oxygen and nitrogen atom recombination. The first and last lumophors were chosen because of their widely different luminescence response to oxygen atoms, and CaO(#19), i.e., "pure" CaO, was chosen as an intermediate case.

B. Dependence of Atom Luminescence on Duration of Atom Exposure

The initial response for luminescence by atom excitation occurred within 0.5 sec, a value limited by the speed of the recorder pen. The subsequent response depended to some extent upon the lumophor temperature. For example, the subsequent response of CaO:Sb:Cl(#3) and CaO:Bi(#7) to nitrogen atoms depended upon the lumophor temperature in the following way: at 300°K the luminescence dropped to about one-half the initial value in one minute, then remained constant; at 475°K the luminescence was almost unchanged from the initial value; and at 675°K the luminescence increased slowly over a period of 10 minutes to about three times the initial value and then remained constant. The corresponding dependence

with oxygen atoms was obscured by the rapid decrease of luminescence response with time of oxygen atom exposure, a subject which will be discussed in detail below.

Experiments were designed to evaluate the effect of extended atom exposure upon a lumophor. This information was necessary to select optimum conditions for a lumophor to be used as an atom probe. The study was focused almost entirely on the effect of oxygen atoms on CaO:Sb:Cl(#3). The effect of nitrogen atoms was studied only to a limited extent because the luminescence intensity essentially remained constant with nitrogen atom exposure.

1. Effect of Exposure to Oxygen Atoms

When oxygen atoms excite luminescence in CaO lumophors, the luminescence intensity L is found to decrease with time t according to the relationship $L = t^{-\epsilon}$, where ϵ is a constant. The value of ϵ, obtained from the slope of a log-log plot, is subsequently referred to as the luminescence "exponential" and is used as an index of the rate of luminescence decrease. Under certain circumstances the curves exhibit two distinct slopes with "initial" and "final" exponentials (shown in parentheses in Fig. 5). The exponentials of these curves and the "break-time" (the time to the point of intersection of the two curves after the discharge was initiated) were found to be mutually related and to depend upon several parameters.

In order to understand the mechanism of the luminescence decrease and to find means of minimizing it, it was of interest to compare the effect of exposure of oxygen atoms on the various energy transfer parameters. The results of the effect of oxygen atom exposure on luminescence intensity, heat generated, and recombination coefficient are shown in Fig. 5 for an experiment in which a break was observed, i.e., for a freshly baked lumophor sample. The exponentials of the heat and recombination coefficient curves are also shown in parentheses. Since the total oxygen pressure was 16μ, a pressure regime in which atom transport occurs in the present geometry in the transition from molecular to

viscous flow, the recombination coefficients calculated according to the usual analysis[9] are only relative values γ_L'', and the changes in γ_L'' due to oxygen atom exposure are also relative. From Fig. 5 two important observations can be made: (1) the time at which the break in the curves occurs appears to be the same for L, H, and γ_L'', and (2) up to the break the values of H and γ_L'' are essentially constant while that of L decreases rapidly.

For experimental conditions under which no break was observed in L, i.e., for a lumophor aged after the baking process, no break was observed in H (Fig. 6) or in the absolute value of γ_L' (Fig. 7) obtained at an oxygen pressure of 27μ, in the viscous flow regime for which the necessary theory applies.[9]

The initial and final exponentials and the break-times are tabulated in Table III for several values of discharge power and under various treatments of the lumophor after it was baked (at 800°K for 10 min) and prior to the exposure to oxygen atoms. The temperature of the CaO:Sb:Cl(#3) was 400°K and the oxygen pressure was 16μ during the time that the discharge was operated. It will be noted that the value of the initial exponential is less than or approaches that of the final exponential, which is essentially constant. The break-time decreases for conditions of (1) high atom density, i.e., high discharge power, and (2) long periods of time between the bake and the initial exposure to atoms (sum of the times in vacuum and in O_2, Table III).

It was found that the temperature at which the lumophor was originally baked (10 min in vacuum) affected the initial exponential. The initial exponential was found to be -0.93, -0.88, and -0.69 corresponding to bake temperatures of 730°, 775°, and 800°K (discharge power 130 watts in oxygen at a pressure of 16μ). The significant change in exponentials occurs between 775° and 800°K, and within the observation period of 60 min a break in the exponentials was observed only for the lumophor baked at 800°K.

The luminescence intensity and the luminescence decrease appear to be confined to a superficial depth of the powdered lumophor. This was

demonstrated by gently stirring a lumophor after its luminescence intensity had decreased by a factor of 50 due to oxygen atom exposure. The luminescence response of the stirred lumophor was found to be equivalent to the original sample. The stirring was done in air at atmospheric pressure, and it was established that the exposure to air without stirring did not restore the luminescence response.

It is of interest to evaluate a lumophor for use as an atom probe under conditions comparable to those expected in the upper atmosphere. Since the present equipment could not be readily adapted for quantitative analysis of low atom densities at pressures less than about 10μ, a qualitative study was made to determine the relative effect of oxygen pressure and discharge power on luminescence response. Low absolute atom densities were achieved at high pressures by reducing the discharge power. The results are shown in Fig. 8 as a log-log plot of luminescence intensity versus atom exposure time for the oxygen pressures 27 and 0.25μ, and luminescence exponentials are indicated in parenthesis. For these conditions under which low absolute atom densities prevail the initial exponentials are small compared with those in Table III.

The effect of lumophor temperature on the luminescence intensity and exponentials is shown for CaO:Sb:Cl(#3) in Fig. 9 and for CaO:Mn:Cl(#4) in Fig. 10 for constant discharge power. The luminescence intensity, after 1 min exposure to oxygen atoms, reaches a maximum in the temperature interval of 400° to 575°K.

Under certain circumstances the luminescence intensity about 0.1 sec after initiation of discharge was about 10 times greater than that absorbed at 1 min. This behavior, which was not studied in detail, was observed to occur when the lumophor temperature was as high as 675°K, or when the lumophor had been heated at 475°K for a period of about 1 hour in oxygen at a pressure of 45μ. In these cases the intensity decreased rapidly, within a minute, to the values shown in Figs. 9 and 10.

The effect of temperature on the initial exponential (after 1 min) is shown in Fig. 11. It may be noted that luminescence bands used for the measurements are peaked at 4000A for CaO:Sb:Cl(#3) and at 6000A for CaO:Mn:Cl(#14).

A material reduction in luminescence response was observed when the lumophor CaO:Sb:Cl(#3) was subjected to the following sequence of steps: (1) exposure to atomic oxygen for various periods of time, (2) evacuation and heating (baking) at 800°K for 10 min, (3) cooling to 400°K, and (4) exposure to oxygen atoms to compare luminescence response before and after the bake. Steps 2 and 3 required a total time of 30 min. The results, summarized in Fig. 12, indicate that the reduction in luminescence response depends upon the exposure time to oxygen atoms and upon the baking process; as little as 8 seconds exposure to oxygen atoms produced a noticeable effect. It was noted in a control experiment that very little decrease in luminescence response was produced when a lumophor was stored in vacuum at 400°K for 30 min after the initial oxygen atom exposure but with no baking. Also the effect of the short duration (8 sec) exposure to oxygen atoms was found to prevail even after 2 hours evacuation of such a treated lumophor prior to baking.

2. Effect of Exposure to Nitrogen Atoms

The response of various lumophors to nitrogen atom recombination has been discussed in detail,[6-8] but the response of CaO:Sb:Cl(#3), which was used in the current research in connection with oxygen atom recombination, had not been examined previously. The relative luminescence intensities of this lumophor excited by nitrogen atoms were 1, 8, and 12 at lumophor temperatures of 300°, 475°, and 675°K; the luminescence intensity remained essentially constant for the duration of atom exposure of about 120 min.

In contrast to expectation from the earlier work[6-8] the intensity of the 4000A band of CaO:Sb:Cl(#3) did not change appreciably with exposure time at 300°K. Re-examination of CaO:Bi(#7) at 300°K likewise showed no decrease of the 4200A band, although it had been observed earlier.[7] The absence of a decrease of luminescence in present work is attributed to the "cleaning" effect on the apparatus by oxygen atoms.

3. Alternate Exposure to Oxygen and Nitrogen Atoms

The effect of alternate exposure to oxygen and nitrogen atoms is shown schematically in Fig. 13. A decrease of luminescence intensity of

CaO:Sb:Cl(#3) resulted from oxygen atom exposure (Curve A). Subsequent exposure to nitrogen atoms resulted in the expected luminescence response to nitrogen atoms (Curve B). The exposure to nitrogen atoms restored the original response of the lumophor to oxygen atoms (Curve C). Also, the luminescence response to oxygen atoms was not affected by interrupting the discharge for 10 min (Curve C).

In other experiments it was shown that a normal response to nitrogen atoms was observed even for a lumophor whose response to oxygen atoms was markedly decreased by the process of oxygen atom exposure followed by baking.

C. Electron Spin Resonance Studies

The ESR studies were designed to determine: (1) the quantitative relationship between luminescence intensity and atom density, and (2) the minimum atom density detectable by the luminescence of a lumophor excited by heterogeneous recombination of the atoms on its surface. The measurements were confined exclusively to the lumophor CaO:Sb:Cl(#3) which was most extensively studied by various other techniques and which appeared to be among the most sensitive for detection of oxygen and nitrogen atoms. The ESR study was begun with nitrogen atoms in order to establish the technique and to avoid the problems associated with the decreased luminescence response of the solid observed in the presence of oxygen atoms.

1. Nitrogen Atom Densities

The ESR spectrum of nitrogen atoms in the gas consists of three lines of equal intensity and separation,[10] and the center line at g = 2 was used for the atom density measurements. Some difficulty was encountered with structure on the nitrogen lines, an effect possibly arising from "sidebanding" of the narrow nitrogen lines by 100 kc field modulation interaction. However, no such interaction was observed with the oxygen atom lines (g = 1.5) although these lines are equally narrow at a given pressure. If the effect is due to a modulation of the ESR line, the results of first-moment analysis for calculation of spin concentration are valid.[11]

The results of the study of the luminescence of CaO:Sb:Cl(#3) at various total nitrogen pressures and nitrogen atom densities are summarized in Table IV. At selected pressures the nitrogen atom density was varied in a stepwise fashion over the widest possible range by adjusting the power output of the transmitter. The relative nitrogen atom densities $[N]_{rel}$, obtained from the peak-peak height of the ESR derivative curve, were measured simultaneously with the luminescence intensity L. Both $[N]_{rel}$ and L were separately normalized.

The absolute nitrogen atom density $[N]_{abs}$ was computed according to the method presented in Appendix B. For this purpose the value of the first-moment S of a nitrogen atom line and of a given molecular oxygen line were obtained for identical adjustment parameters of the ESR spectrometer (e.g., settings of amplitude modulation, cryostat isolator, and microwave attenuator), and the values of S were normalized to the same gain setting. Evaluation of absolute atom densities was carried out only at high atom densities, and the remaining values were obtained on a relative scale from peak-peak heights of the ESR signal (Table IV).

For correlation of luminescence intensity and atom density it is necessary to know the value of the latter at the lumophor position. This value will be less than at the cavity for which ESR results apply because of the atom concentration gradient developed as a result of atom recombination on the lumophor. The value of atom density at the lumophor position was calculated assuming only diffusive flow according to the treatment of Wise and Ablow,[9] and the results are tabulated in Table IV. These results are plotted in Fig. 14 along with those obtained at pressures of 7 and 17μ. However, at the latter pressures no corrections were made since the calculations are applicable only in the viscous flow regime which for the present geometry obtains at total gas pressures equal to and greater than about 40μ. The contributions of bulk flow and of homogeneous atom recombination were found to be small and were neglected.

At pressures greater than about 1000μ the quartz tube in the vicinity of the lumophor and cavity luminesced a green color, the intensity of which

increased with pressure up to 5 mm for a given discharge power. The origin of the luminescence is not understood but appears to be associated with species originating in the discharge.

The recombination coefficient of nitrogen atoms on quartz γ_N was obtained by measurement of the nitrogen atom density profile in the 10 mm o.d. quartz tube. For this purpose the magnet-cavity assembly was moved stepwise along the quartz tube, and the $[N]_{rel}$ was determined for a series of cavity locations expressed in terms of a distance x between center of cavity and the mouth of the 10 mm quartz tube (R, the radius of the tube was 0.40 cm). For $x < 4$ cm ($x/R < 10$) the magnetic field of the 12-inch magnet associated with the spin resonance equipment interacted with the plasma and affected the atom density. Consequently the data used in the determination of γ_N were obtained at $x/R \geq 10$. A discharge of about 100 watts was established at a total pressure of 75μ in a static system. The analysis of the experimental results was based on a model of atom diffusion in an infinitely long cylinder,[12] and a diffusion coefficient[13] $D_{N,N_2} = 2.37 \times 10^3$ cm^2 sec^{-1} at 300°K. The value of γ_N was found to be 1.6×10^{-5}, in good agreement with other reported values.[14,15]

2. Oxygen Atom Densities

The ESR spectrum of oxygen atoms[16] in the gas is centered at g = 1.5 and consists of four lines due to Zeeman transitions in the ground state $^3P_2$ and two weak lines, symmetrically placed on each side of the four lines, arising from the magnetic levels of $^3P_1$ (Fig. 15). The relative oxygen atom density was determined by measuring the peak-peak height of the ESR derivative curve for transition d (Fig. 15) using low modulation amplitude. Absolute oxygen atom density $[O]_{abs}$ was obtained from first-moment analysis of (1) the modulation broadened lines, transitions a to f, and (2) of the six resolved lines using low modulation amplitude. The results of these two methods agreed to within ± 5%. The method of calculating absolute oxygen atom densities from first-moments is discussed in Appendix B.

The relationship between oxygen atom density [O] and luminescence intensity of CaO:Sb:Cl(#3) was studied at a single pressure, 16μ, the

lowest pressure at which the discharge power could be operated over a large range. Because of the decreased lumophor response with time of exposure to atoms two types of experiments were carried out. In the first (80 min) the atom density was maintained at a high value (5.4×10^{13} oxygen atoms/cc), except when it was decreased stepwise over a period of about 1 min and the luminescence intensity and atom density were simultaneously recorded. In this manner the results at 1, 4, and 26 min exposure time were obtained. These results show the non-steady-state relationship between luminescence intensity and atom density (Table V a). Subsequently, under steady state conditions, the same lumophor was exposed to various constant atom densities. From these measurements the change of luminescence response with fixed atom densities could be examined (Table V b). The relative oxygen atom densities $[O]_{rel}$ in Table V were recorded by adjusting the ESR spectrometer for a peak of the derivative of an oxygen line (transition d). Conversion of these data to absolute oxygen atom densities $[O]_{abs}$ was made from the calibration results presented in Table VI and from the values of $[O]_{rel}$.

Graphical presentation (Fig. 16) of the experimental results in Table V a shows that the luminescence intensity is approximately proportional to $[O]_{abs}$. From the data presented in Table V b it can be seen that at atom densities equal or less than 9×10^{11} atoms/cc the luminescence intensity shows no time variation. The horizontal arrows in the luminescence intensity column of Table V b indicate the extent of change of response during the appropriate time interval for higher atom densities.

It was of considerable interest to account for the unexpectedly large luminescence response and the stable luminescence with time for small atom densities (Table V b). In this connection it was noted that the color and intensity of the oxygen discharge varied from a faint yellow at low discharge power to a bright blue at high power. As the discharge power was increased the light intensity of the discharge increased somewhat abruptly at a value which also corresponded to the onset of a luminescence response which decreased upon atom exposure (Table V b).

The determination of oxygen atom density by the ESR resonance absorption due to atomic oxygen $[O]_{abs}$ was supplemented with measurements of the change in the molecular oxygen density evaluated from the decrease of the ESR resonance absorption due to molecular oxygen $[O]_{O_2}$ (Table VI). As will be noted from Table VI, the ESR signal due to the disappearance of O_2 is much larger than that due to the appearance of atomic oxygen. It must be concluded that the discharge produces other species than ground state atomic oxygen (^3P). For example, excited atomic and molecular species such as the atomic states ^1D and ^1S and the molecular states a $^1\Delta$ and $b^1\Sigma g^+$ would not be detected because they have no spin resonance. The electronically excited species $^1\Delta_g$ is known to be metastable and to be produced in high concentrations by an electrical discharge in oxygen.[17]

It was established that the population of the ^3P states of oxygen atoms was not affected by discharge power; hence, the density of ground state atoms could be measured from any of the atomic ESR lines (Fig. 15).

The recombination coefficient of oxygen atoms on quartz was obtained by the method previously discussed for nitrogen atoms. The data were taken at a total pressure of 66μ at which the diffusion coefficient[14] D_{O,O_2} is 4.0×10^3 cm^2 sec^{-1} at 300^{0}K. The results yield a recombination coefficient of $\gamma_O = 1.0 \times 10^{-4}$, in good agreement with reported values.[18,19]

The luminous flux emitted by CaO:Sb:Cl(#3) excited by oxygen atoms was estimated from the photocurrent produced under given conditions and from the corresponding luminous sensitivity of the photomultiplier for the optical system associated with the ESR apparatus (Fig. 3). The maximum anode current resulting from atom luminescence was about 10^{-4} amps for the K 1306 photomultiplier operated at 95 volts per stage. The manufacturer (Dumont) quotes the average luminous flux for the above operating voltage as 5 amps/lumen (color temperature 2870^{0}K). Therefore the luminous flux emitted by the lumophor was (10^{-4} amps)/(5 amps/lumen) or 2×10^{-4} lumens.

DISCUSSION

In this section are discussed (1) the interactions between atoms and lumophors with particular reference to the problems associated with quantitative analysis of atom densities, and (2) the mechanisms of atom-excited luminescence and reduced luminescence response resulting from exposure to oxygen atoms.

A. Quantitative Analysis of Atom Densities

The minimum atom density detectable by atom-excited luminescence can be estimated from the ESR atom density measurement and the signal/noise ratio (S/N) of the associated luminescence intensity. In this treatment the minimum detectability is taken to be equal to the noise level of the luminescence signal. Based on the data in Table V one finds a minimum detectability of 6×10^{11} oxygen atoms/cc for the case of $[O]_{abs} = 1.2 \times 10^{13}$ atoms/cc and a S/N = 20 for the luminescence intensity. The particular example was chosen because it represents a freshly prepared lumophor and the conditions under which the S/N could be precisely evaluated. In like manner, the minimum detectability for nitrogen atoms is estimated to be 2×10^{12} N atoms/cc for the case of $[N]_{abs} = 2.8 \times 10^{13}$ atoms/cc and a S/N = 18. Therefore, the minimum atom density detectable by atom-excited luminescence of CaO:Sb:Cl(#3) is about 1×10^{12} atoms/cc for oxygen and nitrogen atoms. Several improvements in the sensitivity appear possible: a factor of 10 by increasing the operating voltage of the photomultiplier; a factor of 100 by cooling the photomultiplier to reduce dark noise; and a factor of 100 by increasing lumophor area, improving optics, and increasing the electronic response-time constant. It remains for future work to determine whether at such low atom densities the kinetics of atom-excited luminescence remains first order. For example, at sufficiently low atom density the surface coverage will not be complete and the kinetics of atom recombination may approach second order.

The minimum detectable atom density by an ESR measurement may be estimated from the ESR atom density at some conveniently low value and

the signal/noise ratio for this measurement. For nitrogen atoms the data at a pressure of 7μ (Table IV) lead to a detectability of (2.8×10^{13}) $(1/300) = 7 \times 10^{10}$ nitrogen atoms/cc. For oxygen atoms the data at a pressure of 16μ (Table VI) lead to a detectability of $(0.33 \times 10^{13})(1/170)$ $= 2 \times 10^{10}$ oxygen atoms/cc. These detectabilities for nitrogen and oxygen atoms are considered to be comparable. By increasing the integrating time (response time) of the ESR spectrometer from the value of 0.3 sec used in the present work to 10 sec, detectability may be improved by a factor of about 6, e.g. $(10/0.3)^{\frac{1}{2}}$. Thus the limit of detectability is found to be 7×10^9 atoms/cc, a value which agrees with the theoretical estimate by Sands,[20] i.e., the minimum number of spins $n_s = 2 \times 10^{11}\ \Delta H$, where ΔH represents the line width. For the atomic lines of oxygen (transition d) and of nitrogen, ΔH is about 0.02 gauss at a pressure of 20μ, and n_s is 4×10^9 spins.

The agreement between experimental and theoretical detectabilities strongly supports the quantum mechanical method of evaluating atom densities.

B. The Lumophor as a Probe of Atom Densities

The suitability of a probe to measure atom densities depends upon the sensitivity of atom detection, which was discussed above, and also upon the lumophor's time response and ability to distinguish atoms of different kinds.

It may be possible to distinguish between oxygen and nitrogen atoms by means of atom-excited luminescence of solids. The primary basis of identification is that oxygen atoms excite only CaO lumophors to intense luminescence, whereas nitrogen atoms excite CaO as well as other lumophors. For additional criteria one may employ the luminescence spectra and their temperature dependence which for some lumophors distinguish the two atoms. However, for measurement of oxygen atoms in the presence of nitrogen atoms the differences in spectral response are too small to be of practical importance because in general the response to nitrogen atoms is much greater than for oxygen atoms.

The luminescence response of a lumophor upon alternate exposure to nitrogen and oxygen atoms (Fig. 13) indicates that oxygen atoms do not lower its response to nitrogen atoms. Also, nitrogen atoms appear to "rejuvenate" a lumophor whose response has been reduced by oxygen atom exposure.

In our apparatus the measurement of the time response of the lumophor to a flux of atoms produced when the discharge was initiated for either oxygen or nitrogen atoms was limited by the response time of the recorder, about 0.5 sec, connected to the photomultiplier. The response time is probably much smaller than 0.5 sec. Its determination may be further limited by the time required for oxygen or nitrogen atoms to diffuse from the discharge to the lumophor (Fig. 1), calculated to be about 0.1 sec for a total gas pressure of 20μ.

For sustained exposure to a constant flux of nitrogen atoms the two lumophors, CaO:Sb:Cl(#3) and magnesium tungstate, established essentially constant luminescence intensity over a period of at least one hour. Sustained exposure of CaO lumophors to oxygen atoms resulted in a decrease of luminescence intensity with time, except at low atom densities (which will be discussed separately). From the relationship between the luminescence intensity L, the exposure time t, and the luminescence exponential ϵ, i.e., $L = t^{-\epsilon}$, the rate of decrease of luminescence intensity is given by

$$-\frac{dL}{dt} = \epsilon t^{-(\epsilon+1)}$$

which indicates that dL/dt will become smaller with increasing exposure time. Therefore the response of a lumophor may be made more stable by prior exposure to oxygen atoms, however, with some sacrifice of luminescence intensity. It is also desirable to have a low initial luminescence exponential, which is associated with a large break-time, as can be achieved by baking of the lumophor just prior to oxygen atom exposure (see Table III).

The initial luminescence exponential is reduced essentially to zero at low atom densities, as obtained in our apparatus at low discharge power or total gas pressures (Fig. 8). However, this effect may be due to

excited atomic or molecular species produced by the discharge. In this connection it was noted that the color of the discharge in oxygen was different for low and high discharge powers. Further evidence of excited species may be found in a comparison of oxygen atom densities by the ESR techniques involving oxygen-atom and oxygen-molecule resonances (Table VI).

The optimum temperature range for CaO:Sb:Cl(#3) as a probe of oxygen atom densities is from 400° to 500°K, a conclusion based on the minimum initial exponential observed in this range (Fig. 11) and the large luminescence response at temperatures close to this range (Figs. 9 and 10).

For nitrogen atoms the luminescence intensity is proportional to nitrogen atom density at the lumophor, CaO:Sb:Cl(#3), in the pressure range of 41 to 290μ. At higher pressures, e.g. at 770μ, the results are of low accuracy because of the low atom density reaching the lumophor and because of the various corrections for the processes which limit atom transport. At still higher pressures up to 5 mm the luminescence of the quartz walls predominates over that of the lumophor. This behavior may be due to the presence of some energetic species other than ground state atoms.

At low pressures of 7 and 17μ an unusually large luminescence response to nitrogen atoms is observed (Table IV and Fig. 14). The atom concentration above the lumophors is somewhat less than that measured at the ESR cavity due to some atom loss by heterogeneous reaction on the quartz walls between cavity and lumophor. However, because the pressure range is in the intermediate region between viscous and molecular flow such a correction is difficult to make from a theoretical point of view. Nevertheless any correction will further reduce the atom density in the vicinity of the lumophor, thereby shifting the curve to a still greater slope in Fig. 14. Perhaps this greater luminescence response for a given nitrogen atom density can be explained by the presence of excited species originating from the discharge, such as the molecular excited species $A\ ^3\Sigma_u^+$ with about 6.2 eV energy (which is sufficient to excite luminescence) and with a radiative lifetime of the order of 1 sec.[21,22] It is estimated[22,23]

that under our experimental conditions the diffusion time of this species is less than its radiative lifetime for pressures less than about 150μ. Loss of this species by wall de-excitation is expected to require even lower pressures.

The dependence of luminescence intensity upon oxygen atom density for the lumophor CaO:Sb:Cl(#3) at 16μ is somewhat difficult to evaluate because of the decrease of luminescence response associated with prolonged oxygen atom exposure. Under these nonsteady state conditions an essentially linear relationship was found (Fig. 16 and Table V a). The oxygen atom density values reported here correspond to those measured at the ESR cavity position. Similar to the case with nitrogen atoms, the correction is expected to be small due to the difference in position of the ESR cavity and lumophor.

C. Probable Mechanisms of Atom-Excited Luminescence and Decreased Response due to Oxygen Atoms

The process by which a lumophor is excited by atom recombination is believed to involve adsorption of atoms on the surface followed by atom recombination by a first-order process with respect to the atom density in the gas.[6-8] The recombination energy is transferred to the solid where vibrational and electronic transitions are excited, and heat and luminescence of the solid are produced. Nitrogen atoms are more effective than oxygen atoms in exciting various kinds of lumophors, and an important reason for this behavior appears to be the greater energy available upon recombination of nitrogen atoms (9.76 eV) than of oxygen atoms (5.1 eV). It might be expected that oxygen atoms would most readily excite lumophors with low excitation energies for luminescence. Although such a requirement may generally be valid, the results in Table I, using photoexcitation as a criterion of the excitation energy, indicate that some other solid state properties must be considered. Also, the catalytic efficiency of the lumophor's surface for atom recombination γ' is not a determining factor as judged from the data on three lumophors (Table II). These considerations lead us to the conclusion that an important process which determines

whether a lumophor is excited by oxygen atoms is related to the efficiency of energy transfer to the luminescence center.

The efficiency of energy transfer will in general depend upon (1) the distribution of the atom recombination energy between the solid and gaseous molecules resulting from atom recombination, and (2) the distribution of the accommodated recombination energy to vibrational and electronic states of the solid.

We shall now discuss some of the solid state properties of a lumophor such as calcium oxide which account, at least in part, for many of the observed results. The mechanisms to be discussed are not intended to be comprehensive but rather a guide for future work.

Due to the method of preparation of the lumophor the solid is enriched in anion vacancies and electron charge carriers associated with these defects to account for n-type conductivity.[24] Incorporation of such lattice defects in a crystalline solid gives rise to localized energy levels, e.g. luminescence centers, in the forbidden energy gap. Luminescence centers may also result from surface-adsorbed atoms.[25] If this is the mode of formation of luminescence centers, it may explain why color centers have not been detected in CaO and why atom excitation is much more efficient than photoexcitation. In terms of an energy band model the luminescence excitation process is believed to involve the absorption of some of the atom recombination energy by an electron associated with the luminescence center. In CaO it is probable that the energy level of the luminescence center is normally populated. For example, based on the short wavelength limit of photoexcitation[6] the energy level of the luminescence center is estimated to be at least 3.7 eV below the conduction band and therefore below the intrinsic Fermi level since the band gap is 6.7 eV.[26] Alternatively, the excitation of an unpopulated luminescence center may proceed by an exciton mechanism.[27]

Luminescence results during the process in which the excited electron returns to the luminescence center. The luminescence observed as a result

of atom excitation depends upon the composition of the lumophor. For pure CaO only the band peaked at 4000A (3.1 eV) is observed.[6] Addition of intentional impurities, such as antimony, bismuth, or manganese, introduces energy levels above that of the luminescence center of the pure CaO and results in characteristic luminescence at longer wavelengths.

The mechanism of decreased luminescence response of calcium oxide lumophors due to oxygen atom exposure can be interpreted on the basis of the model proposed. The decreased response can be attributed either to a reduction in the catalytic activity for heterogeneous atom recombination or to a change in the processes associated with luminescence excitation. The first possibility that the surface catalytic activity is reduced by destruction of surface sites is ruled out because the atom recombination coefficient of the surface and the heat generated do not change appreciably while the luminescence intensity decreases markedly (Table II and Figs. 5 and 6). The second mechanism has therefore to be considered. Its mode of action is believed to involve charge transfer to adsorbed species at the surface resulting in depletion of the number of effective luminescence centers or reduction in the efficiency of energy transfer to the luminescence centers.

Surface adsorbed oxygen atoms $O_{(s)}$ may react with excess negative charge carriers in a charge transfer process to yield $O^-_{(s)}$. Surface adsorbed oxygen molecules may react in a similar way to produce $O^-_{2(s)}$, but this reaction is of less importance because the electronegativity of the molecules is less than that of the atoms. The formation of gaseous oxygen molecules $O_{2(g)}$ may involve neutral atoms as well as charged species according to

$$O_{(g)} + O_{(s)} \rightarrow O_{2(s)} + Q \qquad (1)$$

$$O_{(g)} + O^-_{(s)} \rightarrow O^-_{2(s)} + Q' \qquad (2)$$

where Q and Q′ are the energies transferred to the solid. However Q′, which is expected to be less than Q by about 1 eV, may not be adequate to excite luminescence. Accordingly, formation of appreciable surface

concentrations of $O^-_{(s)}$, at the expense of $O_{(s)}$, will reduce the luminescence response to oxygen atoms. Desorption occurs according to

$$O^-_{2(s)} \rightleftarrows O_{2(s)} + \theta \qquad (3)$$

$$O_{2(s)} + q \rightarrow O_{2(g)} \qquad (4)$$

where q is the heat of desorption and θ is the electron returned to the lattice.

Reduced luminescence response may therefore be associated with the production of a space charge region, due to the charged adsorbate, adequate to raise the energy levels of the luminescence centers above the Fermi level. This process may be considered as an increase in the p-type conductivity of the surface. Reduced response will also result when anion vacancies diffuse to the surface and react with $O^-_{(s)}$ and lead to lattice incorporation. Such reactions predominate at elevated temperatures, where the diffusion rate in the solid is high, and account for the irreversible decreased luminescence response to oxygen atoms resulting from baking a lumophor after oxygen atom exposure (Fig. 12).

Because of the amphoteric electronic properties[24] of calcium oxide a change to p-type conductivity may occur upon continued exposure to oxygen atoms

$$O_{(g)} \rightleftarrows O^-_{(s)} + \oplus \; . \qquad (5)$$

The surface of such a solid will continue to exhibit catalytic properties for atom recombination (reactions 1 through 4) although perhaps at a different rate since the desorption, step (3), may proceed by

$$O^-_{2(s)} + \oplus \rightarrow O_{2(s)} \; . \qquad (6)$$

However, luminescence can no longer occur since the luminescence centers have by this time been depleted of electrons.

Based on such a mechanism the behavior of nitrogen atoms would be expected to differ from that of oxygen atoms since nitrogen is less electronegative than oxygen, and less surface charge would be developed than for oxygen atoms. The rejuvenation by nitrogen atoms of a lumophor whose response was decreased by oxygen atoms (Fig. 13) is probably due to

a chemical reaction of the sort

$$N_{(g)} + O^-_{(s)} \rightarrow NO_{(g)} + \theta \quad . \qquad (7)$$

Reaction 7 reduces the space charge due to $O^-_{(s)}$ and permits the energy level of the luminescence center to be restored below the Fermi level. When the lumophor is baked subsequent to oxygen atom exposure, anion vacancies diffuse to the surface where they are destroyed by reaction with $O^-_{(s)}$ or $O^-_{2(s)}$. Although nitrogen atoms cannot restore the luminescence response of such a lumophor to oxygen atoms, nitrogen atoms still can easily excite this lumophor because their higher recombination energy permits transfer of energy to luminescence centers at greater depths in the crystal where changes of space charge and depletion of luminescent centers are less likely to occur.

The above model suggests a way to account for the effect of temperature on the initial luminescence exponential (Fig. 11). At temperature greater than about 450°K the increase in the exponentials may be accounted for by a greater diffusion rate of anion vacancies and calcium excesses from the bulk to the surface where the vacancies are incorporated into the lattice. At temperatures less than 450°K the increase in the exponentials may be due to the increased concentration of surface-adsorbed atoms, $O_{(s)}$, which results in increased concentrations of $O^-_{(s)}$ and leads to formation of an increased space charge. A similar temperature dependence of the surface concentration of atoms was reported for nitrogen atoms[6] on CaO and hydrogen atoms[28] on glass.

The simultaneous change in the exponentials of luminescence, heat, and atom recombination coefficient (the break-time in Fig. 5) suggests that a change occurs in the solid state properties of the CaO surface which equally affects these three parameters. Evidence that a solid state property is involved is based on the observation that the break-time is associated with aging of the lumophor after baking (Table III). Also, when the bake temperature, employed prior to exposure to oxygen atoms, was increased from 775° to 825°K the initial luminescence exponential decreased and simultaneously the break in the response curve was observed.

It is suggested that the solid state property which affects the break is due to a defect or dislocation which is produced at sufficiently high baking temperatures and is then annealed at lower temperatures. The behavior of CaO may be analogous in certain respects to that of BaO for which it has been shown that the diffusion of Ba in BaO occurs by different processes depending upon temperature and depth of penetration into the surface.[29] The change in the solid state property may also result from a conversion of the CaO from an n-type to a p-type semiconductor as a result of annealing and oxygen atom exposure.

ACKNOWLEDGMENTS

The authors wish to thank Professor K. Hauffe, Mr. K. Edvard Borbye, and Dr. William J. Fredericks for valuable discussions concerning solid state properties, and Mr. James S. Mills and Mr. David W. Diffenderfer for assistance in connection with the electron spin resonance measurements. Mr. Brian D. King designed the electronic function generator and Mr. John Casalet constructed the unit.

REFERENCES

1. H. Kallmann-Bijl, "Caspar International Reference Atmosphere 1961," North-Holland Publ. Co., Amsterdam, 1961
2. C. A. Barth, "Chemical Reactions in the Lower and Upper Atmosphere," Interscience Publishers, New York, 1961, p. 303
3. J. Kaplan, W. J. Schade, C. A. Barth, and A. F. Hildebrandt, Can. J. Chem. 38, 1688 (1960)
4. "Handbook of Geophysics," United States Air Force, Macmillan 1961, Revised, pp. 8-3, 8-4
5. K. M. Sancier, W. J. Fredericks, and H. Wise, J. Chem. Phys. 30, 1355 (1959)
6. K. M. Sancier, W. J. Fredericks, and H. Wise, J. Chem. Phys. 37, 854 (1962)
7. K. M. Sancier, W. J. Fredericks, J. L. Hatchett, and H. Wise, J. Chem. Phys. 37, 860 (1962)
8. K. M. Sancier, W. J. Fredericks, and H. Wise, J. Chem. Phys. 37, 865 (1962)
9. H. Wise and C. M. Ablow, J. Chem. Phys. 29, 634 (1958)
10. M. A. Heald and R. Beringer, Phys. Rev. 96, 645 (1954)
11. K. Halbach, Phys. Rev. 119, 1230 (1960)
12. W. V. Smith, J. Chem. Phys. 11, 110 (1943)
13. L. Andrussow, Z. Elektrochem. 54, 566 (1950)
14. J. T. Herron, J. L. Franklin, P. Bradt, and V. H. Dibeler, J. Chem. Phys. 30, 897 (1959)
15. T. Wentik, J. O. Sullivan, K. L. Wray, J. Chem. Phys. 29, 231 (1958)
16. A. Abragam and J. H. Van Vleck, Phys. Rev. 92, 1448 (1953)
17. S. N. Foner and R. L. Hudson, J. Chem. Phys. 25, 601 (1956)
18. H. Wise and W. A. Rosser, "Ninth International Symposium on Combustion," Academic Press, Inc., New York, 1963, p. 733-746
19. S. Krongelb and M. W. P. Strandberg, J. Chem. Phys. 31, 1196 (1959)
20. R. H. Sands (Varian Associates), private communication

21. J. F. Noxon, J. Chem. Phys. 36, 926 (1962)
22. E. C. Zipf, Jr., J. Chem. Phys. 38, 2034 (1963)
23. A. Einstein, Z. Elektrochem. 14, 235 (1908)
24. K. Hauffe and G. Tränckler, Zeit. für Physik, 136, 166 (1953)
25. A. N. Gorban and V. A. Sokolov, Opt. and Spectry. (USSR) 7, 478 (1959)
26. J. Janis and L. Cotton, C. R. Acad. Sci. (Paris) 246, 1536 (1958)
27. S. Apher and E. Taft, Phys. Rev. 79, 964 (1950)
28. B. J. Wood and H. Wise, J. Phys. Chem. 66, 1049 (1962)
29. R. W. Redington, Phys. Rev. 87, 1066 (1952)

Table I Survey of lumophor response to photoexcitation and atom excitation[a]

CLASS	LUMOPHOR	PHOTOLUMINESCENCE			ATOM LUMINESCENCE[c]			
		Excitation	Emission		N		O	
		λ	λ	L	λ	L	λ	L
Appreciable atom luminescence	CaO:Sb:Cl (#3)				4000	1	4000	3
	CaO:Mn:Cl (#17)[b]	3800	4800	--				
			5500	--				
		4800	5500	--				
	CaO:Mn:Cl (#14)				5900	3	5900	1
	CaO:Bi (#7)				4000	1	4000	1
					5300	0.8	5400	0.5
	Magnesium tungstate	2950	4850	2	4650	0.1	5500	<0.02
		2200	3500					
	Cadmium borate	3000	6100	0.3	6300	3	6100	0.04
Photoexcitation energy low[c]	Zinc orthosilicate	2900	5300	2	5400	0.1	5500	0.01
		3670	5300	1				
		3900	5300	1				
	Zinc oxide:Zn	3800	5100	3	5000	0.2	nil	
	Zinc sulfide:Cu:Ag	3750	5200	6	5200	0.03	5200	0.03
Photoexcitation energy high	Calcium halophosphate	2850	5800	0.6	5850	0.1	nil	
	Calcium silicate:Pb	2750	6000	0.3	6100	0.1	nil	
	Calcium tungstate	2750	~4900	0.4	4500	0.1	nil	
					5900	0.1		
	Calcium tungstate:Pb	2900	~4900	0.9	4800	0.3	nil	
Photoexcitation energy unmeasurable	CdO	nil			nil		nil	
	BaO	nil			6000	0.3	nil	
	MgO (#75)	nil			4200	0.5	nil	
					5600	0.5		

[a] Wavelengths λ(A) refer to peak of response; intensities of emission and luminescence L are on relative and independent scales. For atom luminescence: total gas pressure 16μ; lumophor temp. 300°K; discharge power 130 watts.

[b] Reference 6.

[c] Value of L taken during first minute of discharge operation.

Table II. Comparison of energy transfer parameters of various lumophors for oxygen and nitrogen atoms. (Total gas pressure 26μ, discharge power 130 watts; lumophor temp. 300°K.)

Parameter	Oxygen atoms			Nitrogen atoms		
	CaO:Sb:Cl(#3)	CaO(#19)	$MgWO_4$	CaO:Sb:Cl(#3)	CaO(#19)	$MgWO_4$
γ'_H, Recombination coeff. from heat[b]	0.01	--	0.02	0.01	0.003[a]	0.01
γ'_L, Recombination coeff. from luminescence[b]	0.02	--	0.02	0.01	0.008[a]	0.01
L, Luminescence intensity (mv)[d]	3	0.08	0.02	1	0.6	0.7
H, Heat rate[c] (Ω/min)	165	115	100	35	60	25

a. Reference (7).

b. γ'_H measured simultaneously with H; γ'_L measured simultaneously with L.

c. Difference in H produced by oxygen and nitrogen atoms probably due to difference in atom concentrations produced by the given discharge power.

d. For oxygen atoms the values of L were taken about 1 min after initiating discharge; for nitrogen atoms the values of L were essentially constant with time.

Table III. Effect of treatment of lumophor CaO:Sb:Cl(#3) excited by oxygen atoms. (Pressure 16μ during atom exposure; lumophor temperature 400°K.)

Discharge power (watts)	Treatment after bake[c] and prior to oxygen atom exposure			Break-time[a] (min)	Luminescence exponential[b]	
	Time in vacuum (min)	Exposure to O_2			Initial	Final
		Time (min)	Press. (μ)			
130	95	135	45	0	-1.0	-1.0
130	30	60	45	0	-0.77	-0.77
130	17	60	45	0	-0.78	-0.78
130	109	1	16	0	-0.81	-0.81
130	108	2	16	0	-0.75	-0.75
130	48	2	16	0	-0.68	-0.68
130	15	1	16	24	-0.47	-0.77
130	33	2	16	29	-0.50	-0.87
30	23	130	45	18	-0.41	-0.92
55	35	30	45	31	-0.51	-1.08
55	16	10	16	38	-0.35	-1.38
35	21	1	16	40	-0.38	-0.87
35	25	5	16	49	-0.30	-1.00

a. Measured from time of initiation of discharge.

b. Luminescence exponential = $\Delta \log L / \Delta \log t$; L is luminescence intensity (mv) and t is time in (min).

c. 10 min at 800°K in vacuum.

Table IV Luminescence intensity of CaO:Sb:Cl(#3) versus total pressure and nitrogen atom density: Absolute atom densities $[N]_{abs}$ determined from the first-moment analysis using molecular oxygen as spin-density reference. Relative atom density determined from peak-peak height of ESR line. Lumophor temp. 400°K.

TOTAL GAS PRESSURE AT CAVITY		FIRST-MOMENT[a] S	NITROGEN ATOM DENSITY			LUMINESCENCE INTENSITY L (mv)
(μ)	(molecules/cc x 10^{-14})		$[N]_{rel}$ At Cavity	$[N]_{abs}$ (atoms/cc x 10^{-13})		
				At Cavity	At Lumophor	
7	2.3	67	36[b]	2.8[d]	--	45[c]
			25	2.0	--	38
17	5.5	145	55	6.0[d]	--	58
			33	3.6	--	41
			15	1.6	--	28
			2	0.2	--	8
41	13	258	80	14[d]	11	70
			57	10	7.7	52
			11	2	1.5	13
77	25	378	103	10[d]	6.4	50
			70	6.8	4.4	35
			46	4.5	2.9	25
			13	1.3	0.8	6
290	93	192	42	7.8[d]	2.5	17
			17	3.2	1.0	5
770	250	7	3	0.3[d]	0.05	3

[a] For molecular oxygen (transition: K, L, J: 1, 2, 1 → 2) S = 65 for a pressure P_{O_2} = 70μ; ESR parameters were the same as for atomic nitrogen.

[b] Signal/noise ratio = 300

[c] Signal/noise ratio = 18

[d] Absolute atom density measurement (*cf.* Appendix B).

Table V. Luminescence of CaO:Sb:Cl(#3) versus oxygen atom densities and as a function of exposure time to atoms. (Pressure 16μ; lumophor temp. 400°K.)

Exposure time (min)	Oxygen atom density at cavity		Luminescence intensity L (mv)
	$[O]_{rel}$ [a]	$[O]_{abs}$ (atoms/cc x 10^{-13})	
	[a]		
1	116	5.4[b]	288
	91	4.1	222
	40	1.9	165
	25	1.2	93[c]
4	130	6.2	120
	96	4.4	102
	55	2.6	69
	30	1.4	45
	10	0.5	18
26	130	6.2	32
	110	5.2	29
	81	3.8	24
	66	3.0	16
	40	1.9	9.0
	30	1.4	7.8
	[b]		
80 - 84	1.5	.070	13
84 - 86	2.0	.094	15
86 - 93	3.8	.18	17 → 14[d]
93 - 110	2.0	.094	15
110 - 120	1.3	.06	10
120 - 129	3.0	.14	15 → 13
129 - 150	9.4	.44	10 → 8
150 - 167	60	2.8	17 → 11
167 - 176	102	4.8	30 → 19
176 - 187	116	5.4	11 → 7

a. Relative atom density obtained from normalized peak-peak height (mm) of ESR line.

b. Value obtained from Table VI.

c. Signal/noise ratio = 20.

d. The horizontal arrow indicates the decrease of L which occurred during the time interval.

Table VI. Absolute oxygen atom densities $[O]_{abs}$ determined from first-moment analysis using molecular oxygen as spin-density reference.[a]

Discharge power (watts)	Spin species[b]	ESR Intensity I (peak-peak, mm)	Gain G	Modulation amplitude M (volts)	First-moment S (cm^3)	Oxygen atoms/cc x 10^{-13}	
						$[O]_{abs}$	$[O]_{O_2}$
75	O	37[c]	4000	1.28	280	0.33	9
75	O_2	100	2000	0.086	2.7_6		
Off	O_2	91.5	2000	0.086	2.8_6		
100	O	84	3200	1.18	760	1.3	10
100	O_2	102	2500	0.083	2.8_6		
Off	O_2	92	2500	0.083	2.7_2		
420	O	98	1000	1.18	930	5.4	19
420	O_2	106	2000	0.083	2.8_9		
Off	O_2	88	2000	0.083	2.5_0		

a. See Appendix B for details of calculation.

b. ESR lines: transitions a to f for O atoms; transition ($K = 1$, $L = 2$, $M = 1 \rightarrow 2$) for molecular oxygen. Total pressure 16μ.

c. Signal/noise ratio = 170.

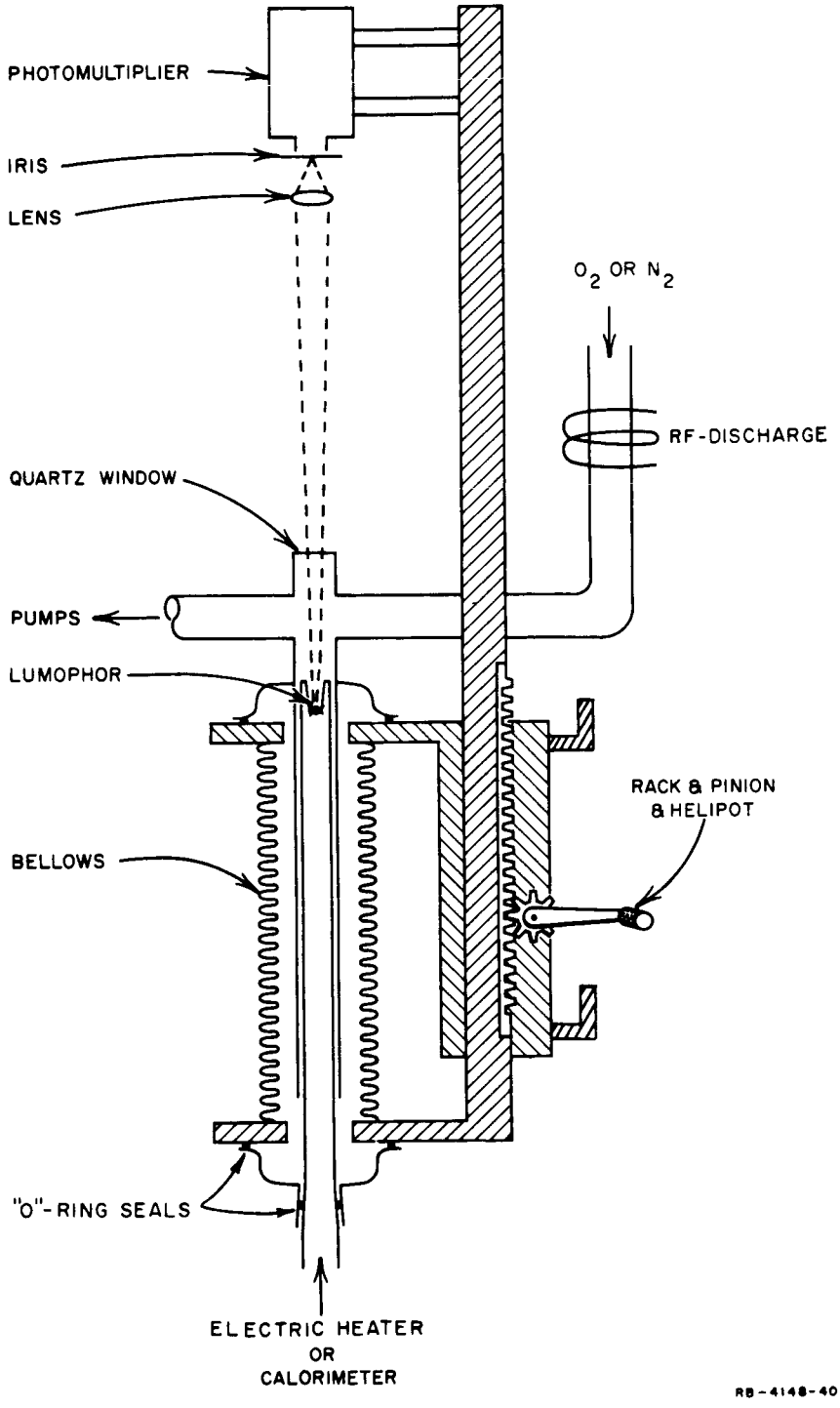

FIG. 1 APPARATUS FOR DETERMINATION OF ATOM RECOMBINATION COEFFICIENT OF LUMOPHORS FROM MEASUREMENTS OF LUMINESCENCE INTENSITY OR CALORIMETRIC HEAT

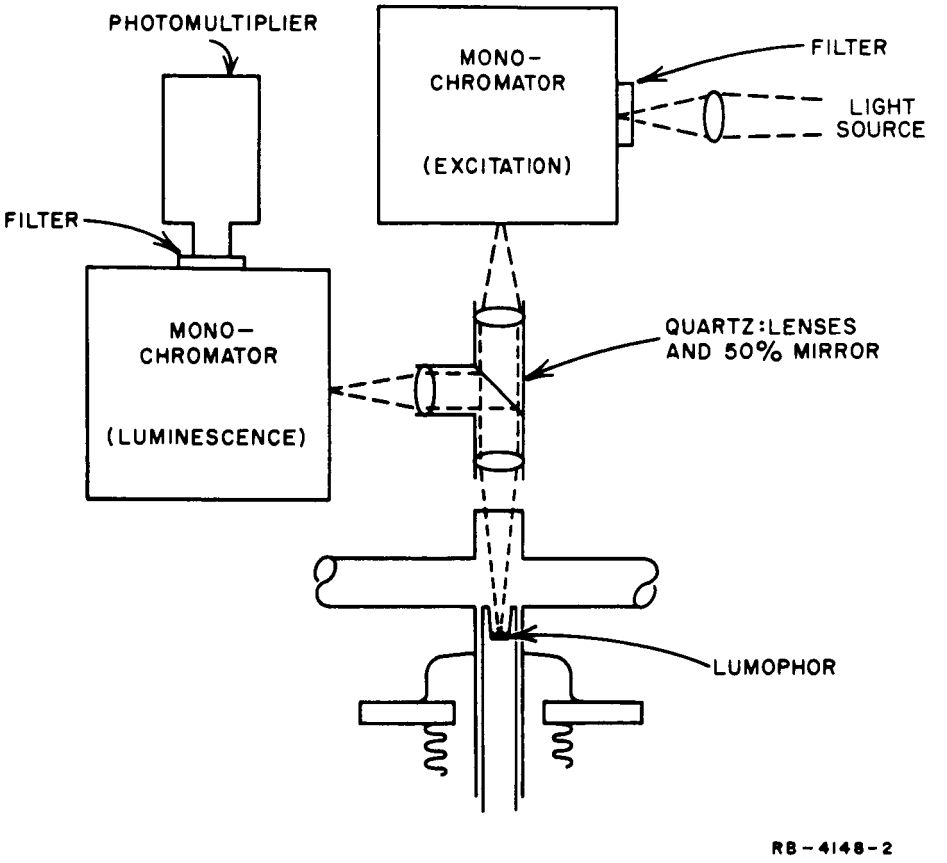

FIG. 2 APPARATUS FOR MEASUREMENT OF PHOTOEXCITATION, PHOTOEMISSION AND ATOM-EXCITED LUMINESCENCE SPECTRA

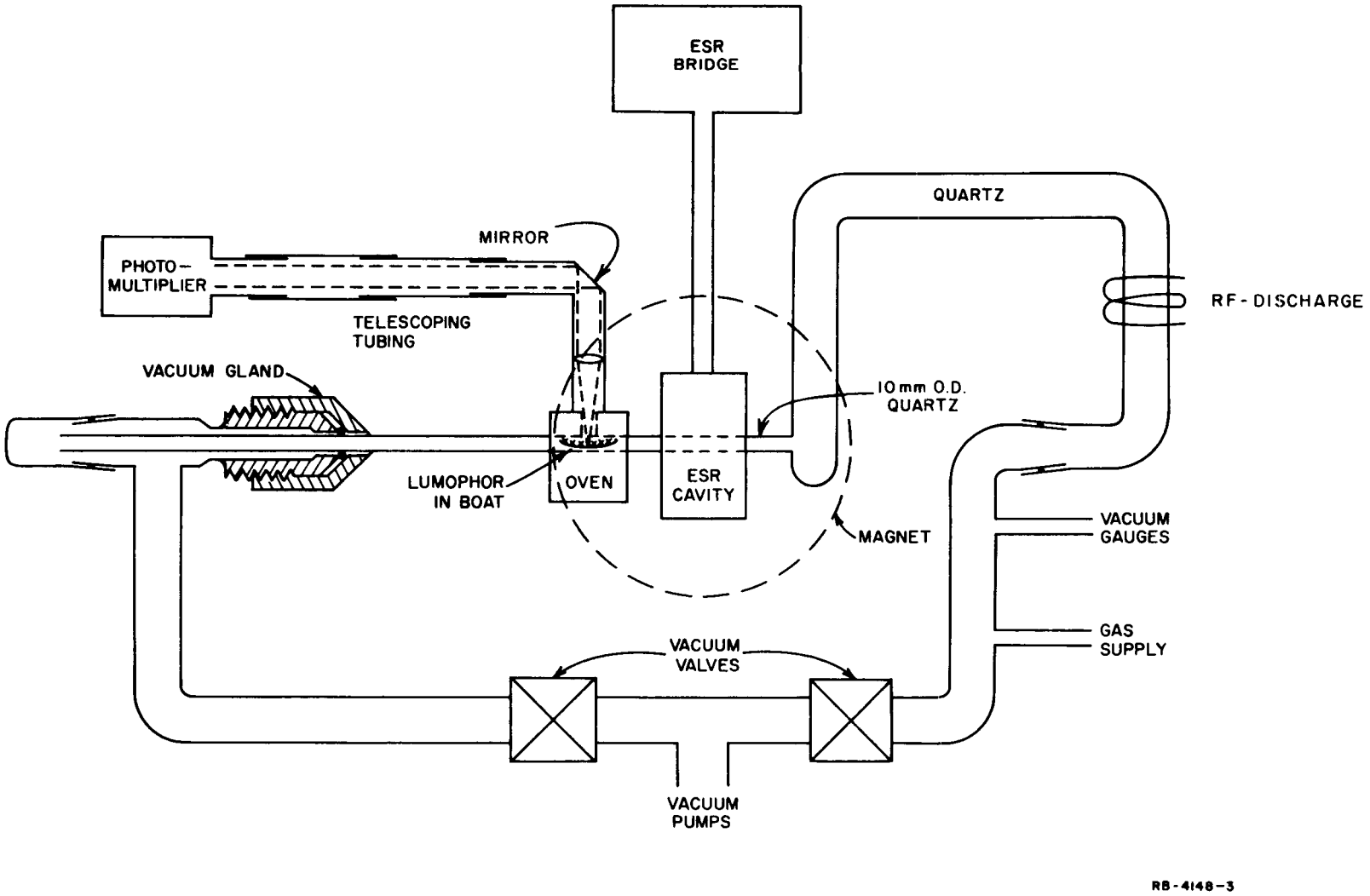

FIG. 3 APPARATUS FOR CORRELATING LUMINESCENCE INTENSITY OF A LUMOPHOR WITH ATOM DENSITY AS MEASURED BY ELECTRON SPIN RESONANCE

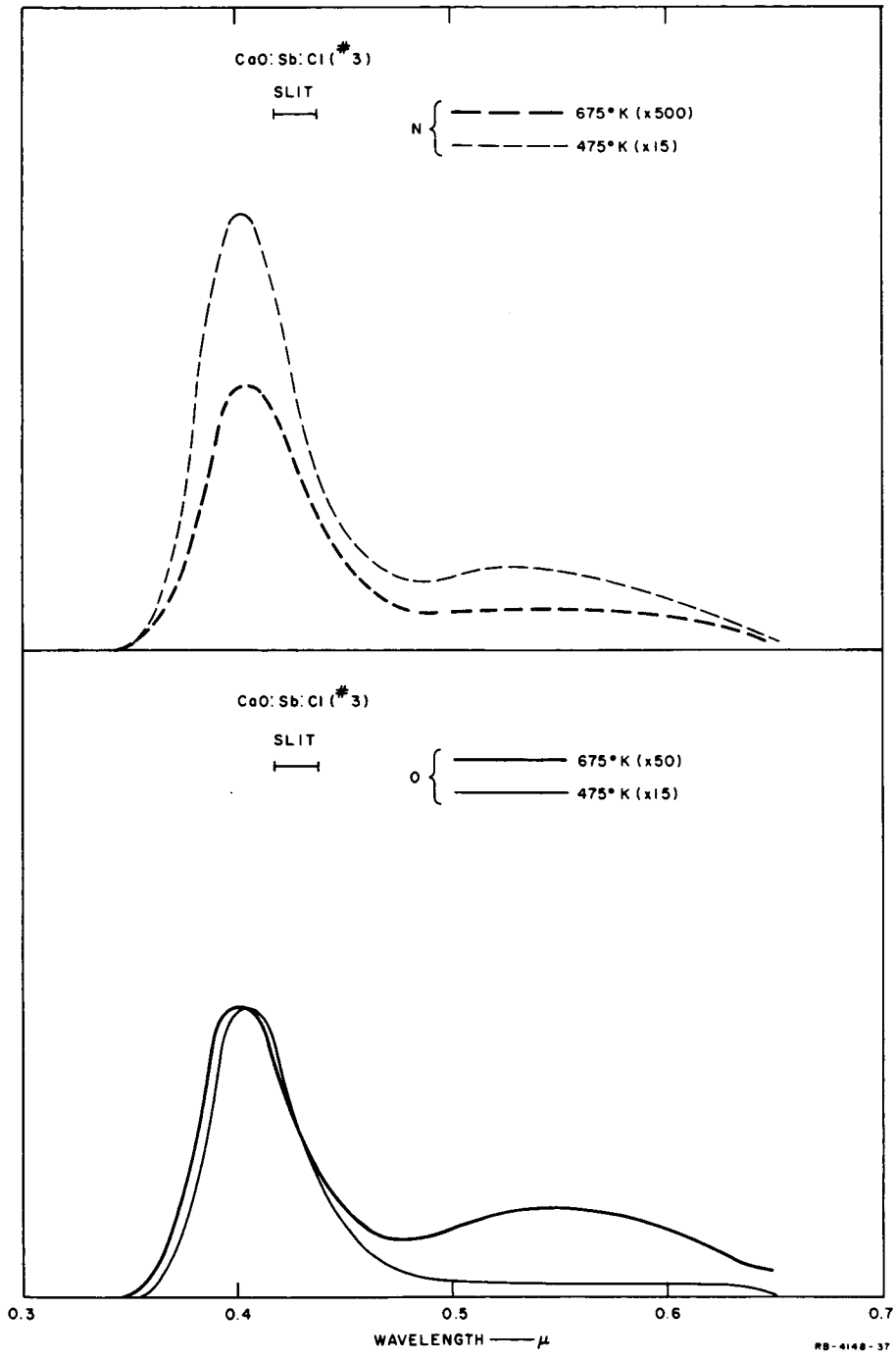

FIG. 4a LUMINESCENCE SPECTRA OF CaO:Sb:Cl(#3) EXCITED BY OXYGEN ATOMS AND NITROGEN ATOMS. RELATIVE ORDINATE SCALE INDICATED BY MULTIPLICATIVE FACTOR IN PARENTHESIS

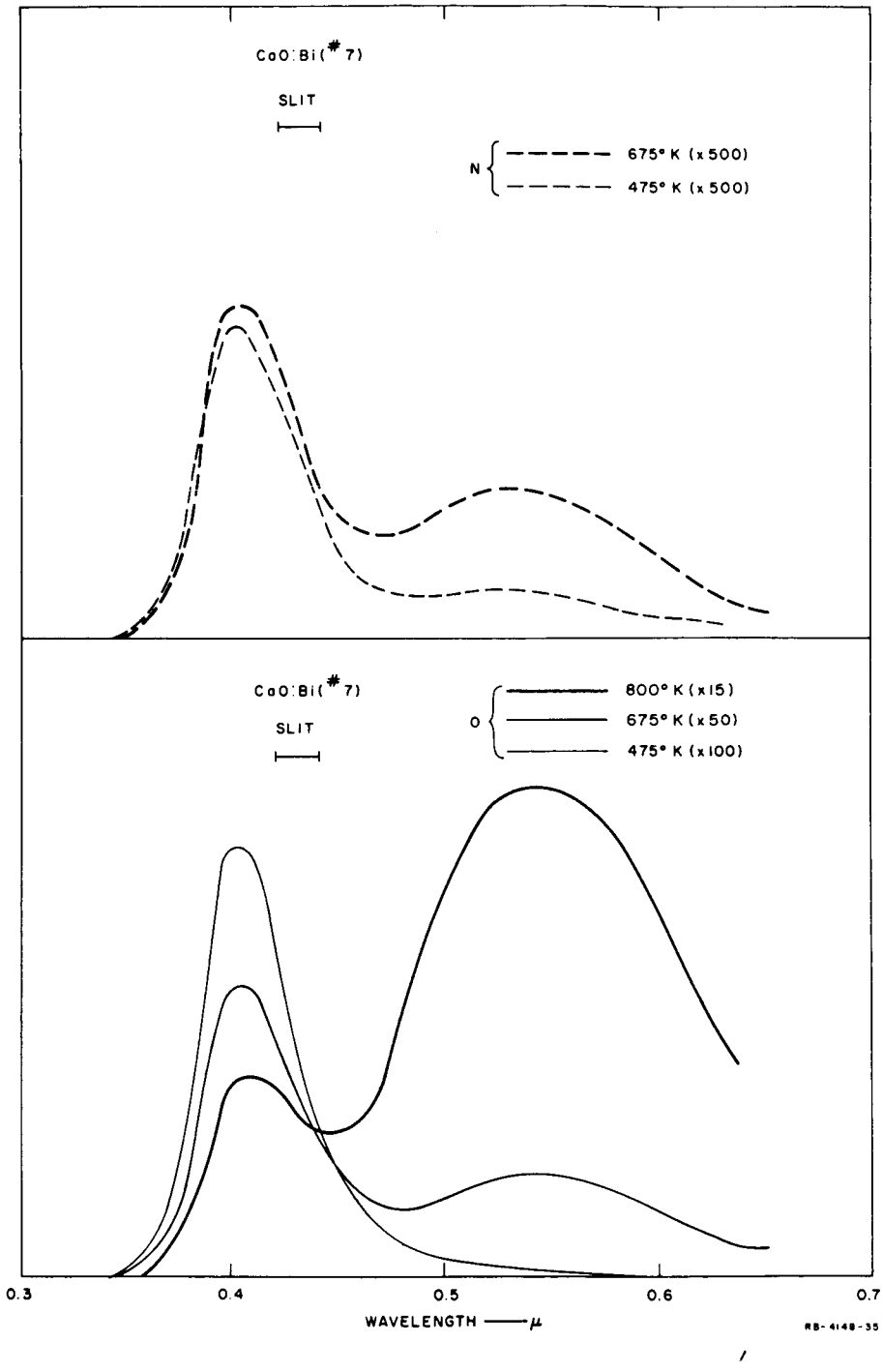

FIG. 4b LUMINESCENCE SPECTRA OF CaO:Bi(#7) EXCITED BY OXYGEN AND NITROGEN ATOMS. RELATIVE ORDINATE SCALE INDICATED BY MULTIPLICATIVE FACTOR IN PARENTHESIS

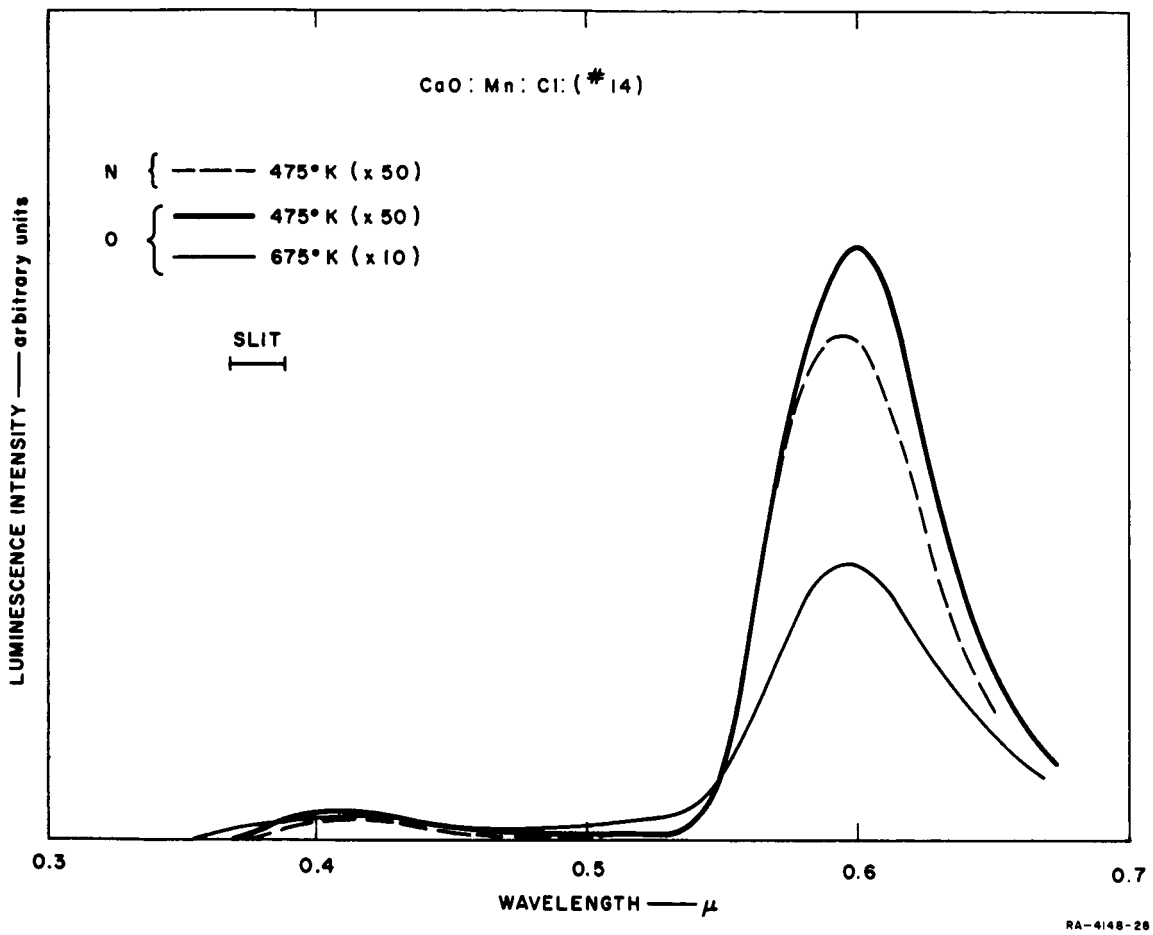

FIG. 4c LUMINESCENCE SPECTRA OF CaO:Mn:Cl(#14) EXCITED BY OXYGEN AND NITROGEN ATOMS. RELATIVE ORDINATE SCALE INDICATED BY MULTIPLICATIVE FACTOR IN PARENTHESIS

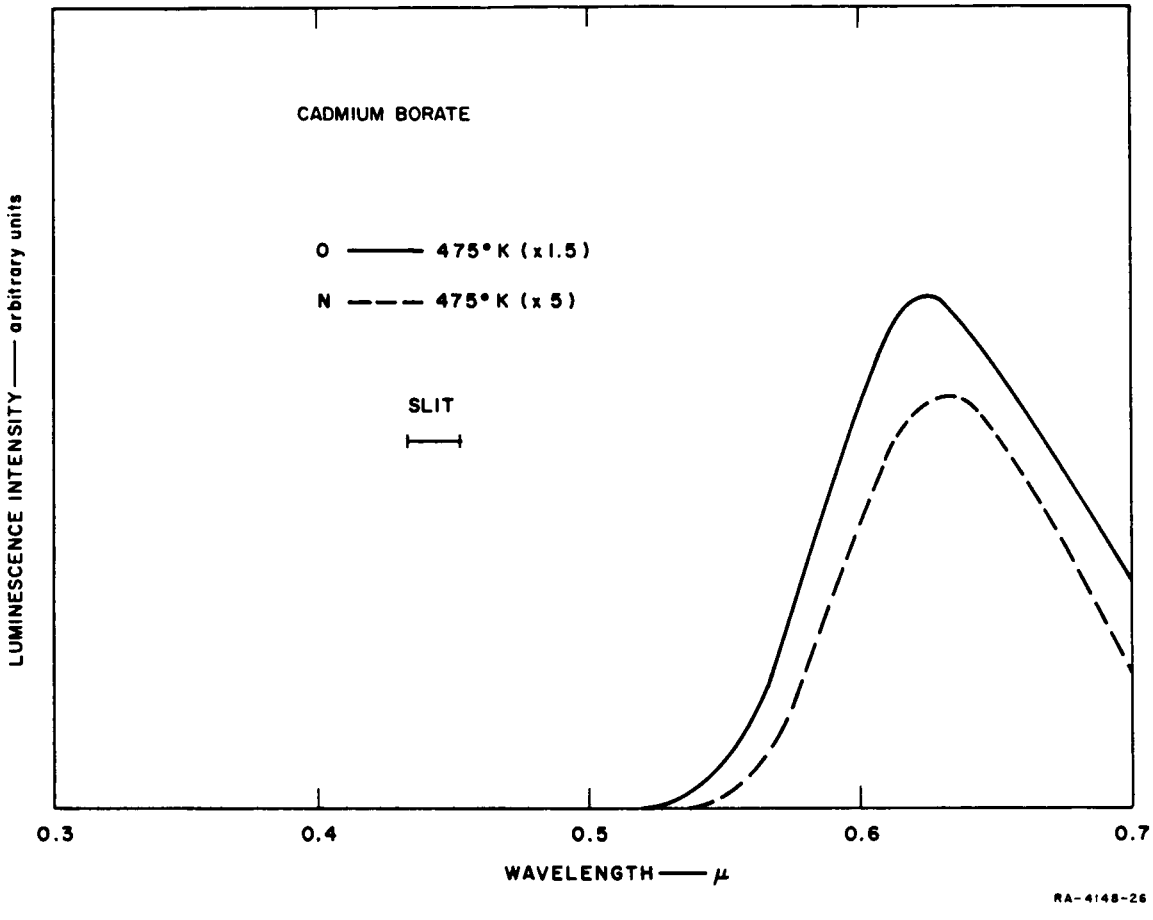

FIG. 4d LUMINESCENCE SPECTRA OF CADMIUM BORATE EXCITED BY OXYGEN AND NITROGEN ATOMS. RELATIVE ORDINATE SCALE INDICATED BY MULTIPLICATIVE FACTOR IN PARENTHESIS

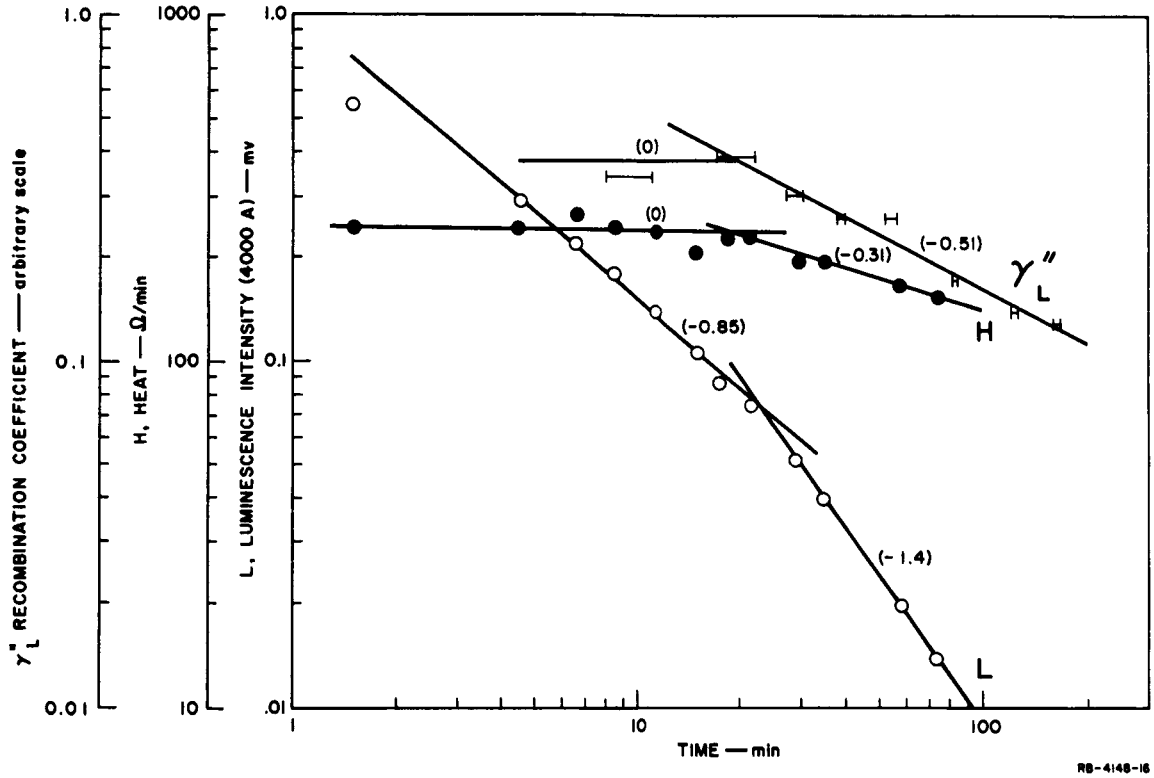

FIG. 5 EFFECT OF TIME OF OXYGEN ATOM EXPOSURE OF FRESHLY BAKED CaO:Sb:Cl(#3) ON THE LUMINESCENCE INTENSITY L AT 4000A, ON THE HEATING RATE H, AND ON THE RELATIVE RECOMBINATION COEFFICIENT γ''_L. DISCHARGE POWER 130 WATTS; PRESS. 16μ; LUMOPHOR TEMP. 400°K. EXPONENTIALS IN PARENTHESES

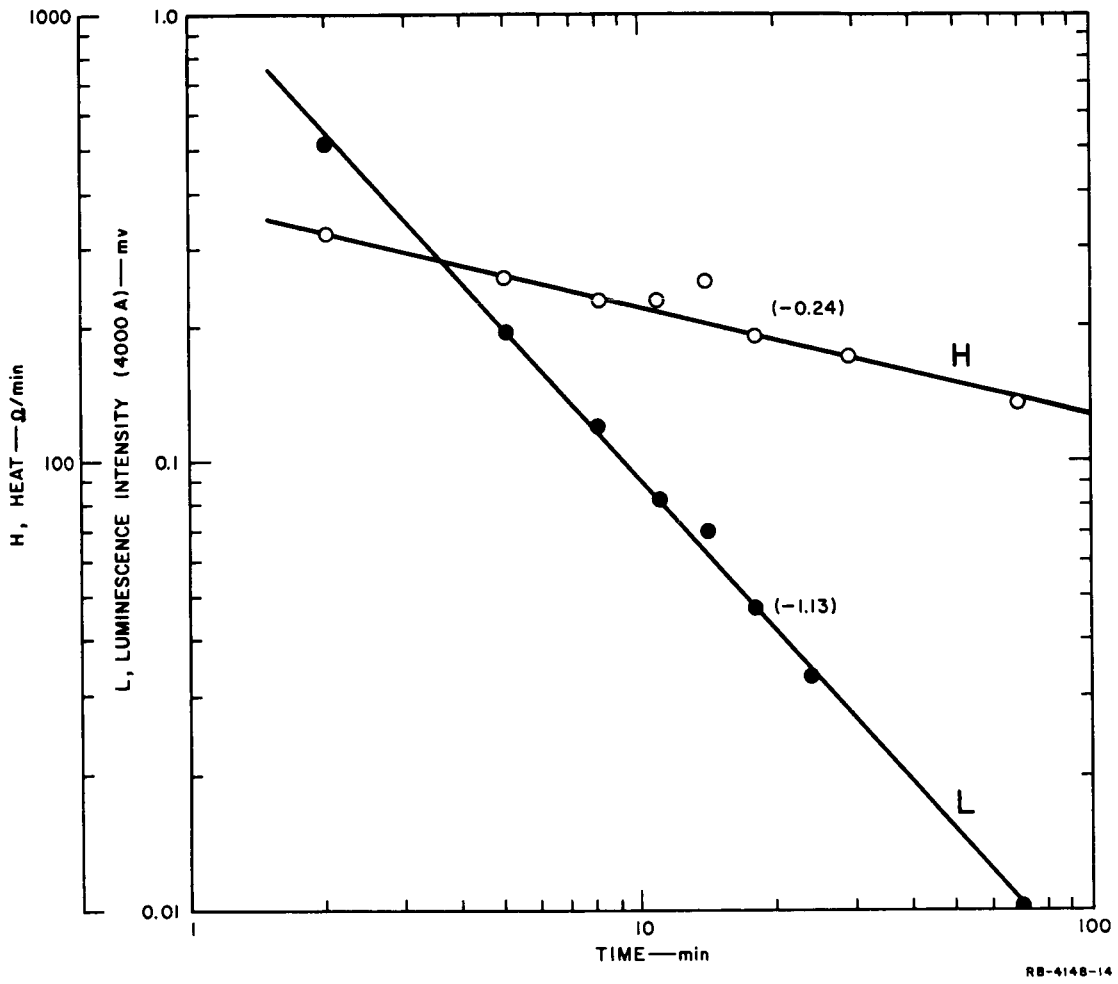

FIG. 6 EFFECT OF TIME OF OXYGEN ATOM EXPOSURE OF AGED CaO:Sb:Cl(#3) ON THE LUMINESCENCE INTENSITY L AND THE HEAT RATE H. DISCHARGE POWER 130 WATTS; PRESS. 16μ; LUMOPHOR TEMP. 400°K. EXPONENTIALS IN PARENTHESES

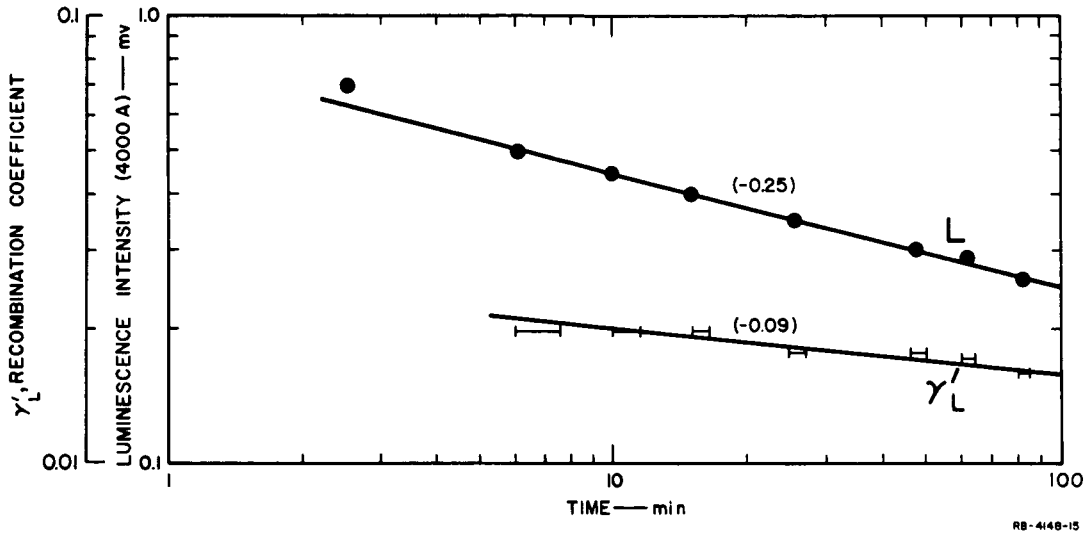

FIG. 7 EFFECT OF TIME OF OXYGEN ATOM EXPOSURE OF CaO:Sb:Cl(#3) ON THE LUMINESCENCE INTENSITY L AND THE RECOMBINATION COEFFICIENT γ'. DISCHARGE POWER 25 WATTS; PRESS. 27μ; LUMOPHOR TEMP. 400°K. EXPONENTIALS IN PARENTHESES

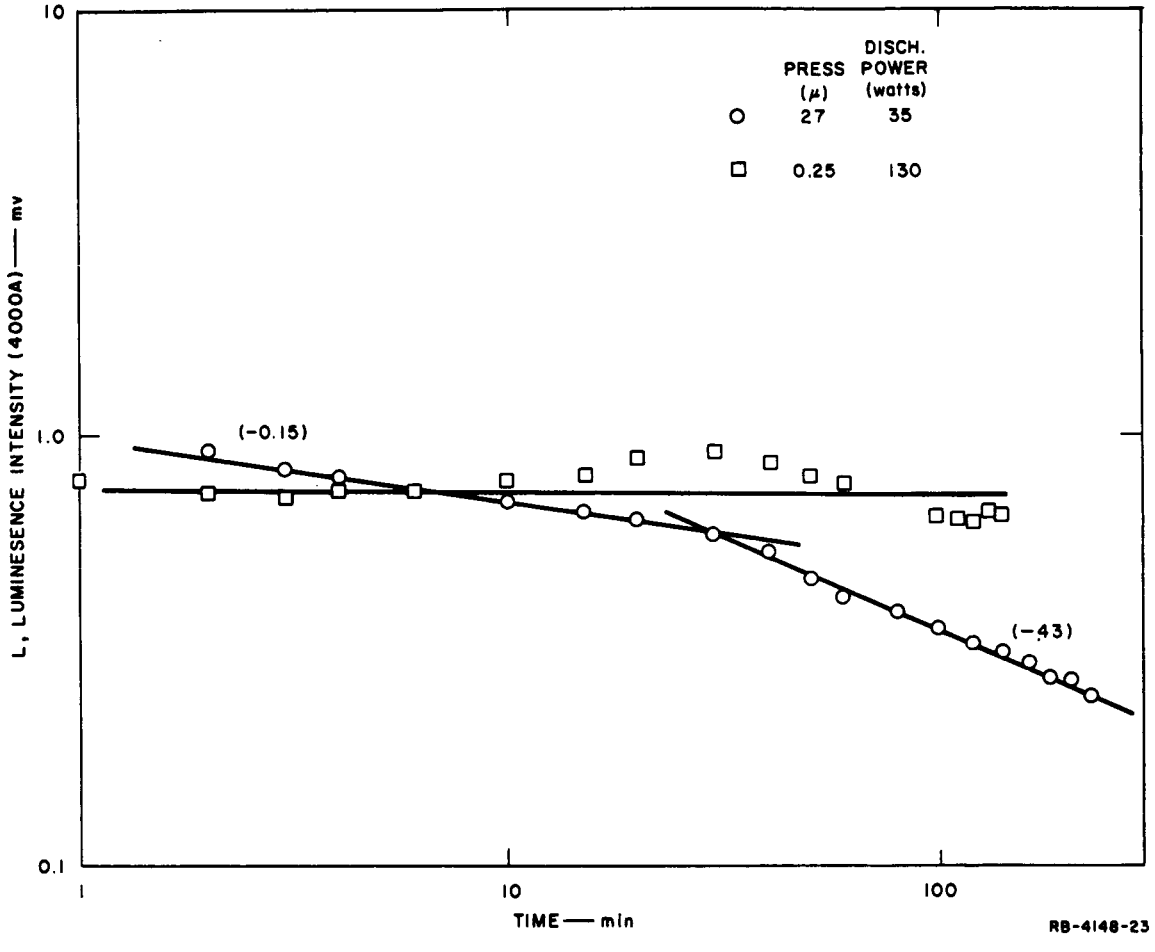

FIG. 8 EFFECT OF TIME OF OXYGEN ATOM EXPOSURE, DISCHARGE POWER, AND TOTAL GAS PRESSURE ON THE DECREASE OF LUMINESCENCE INTENSITY OF CaO:Sb:Cl(#3). LUMOPHOR TEMP. 400°K. EXPONENTIALS IN PARENTHESES

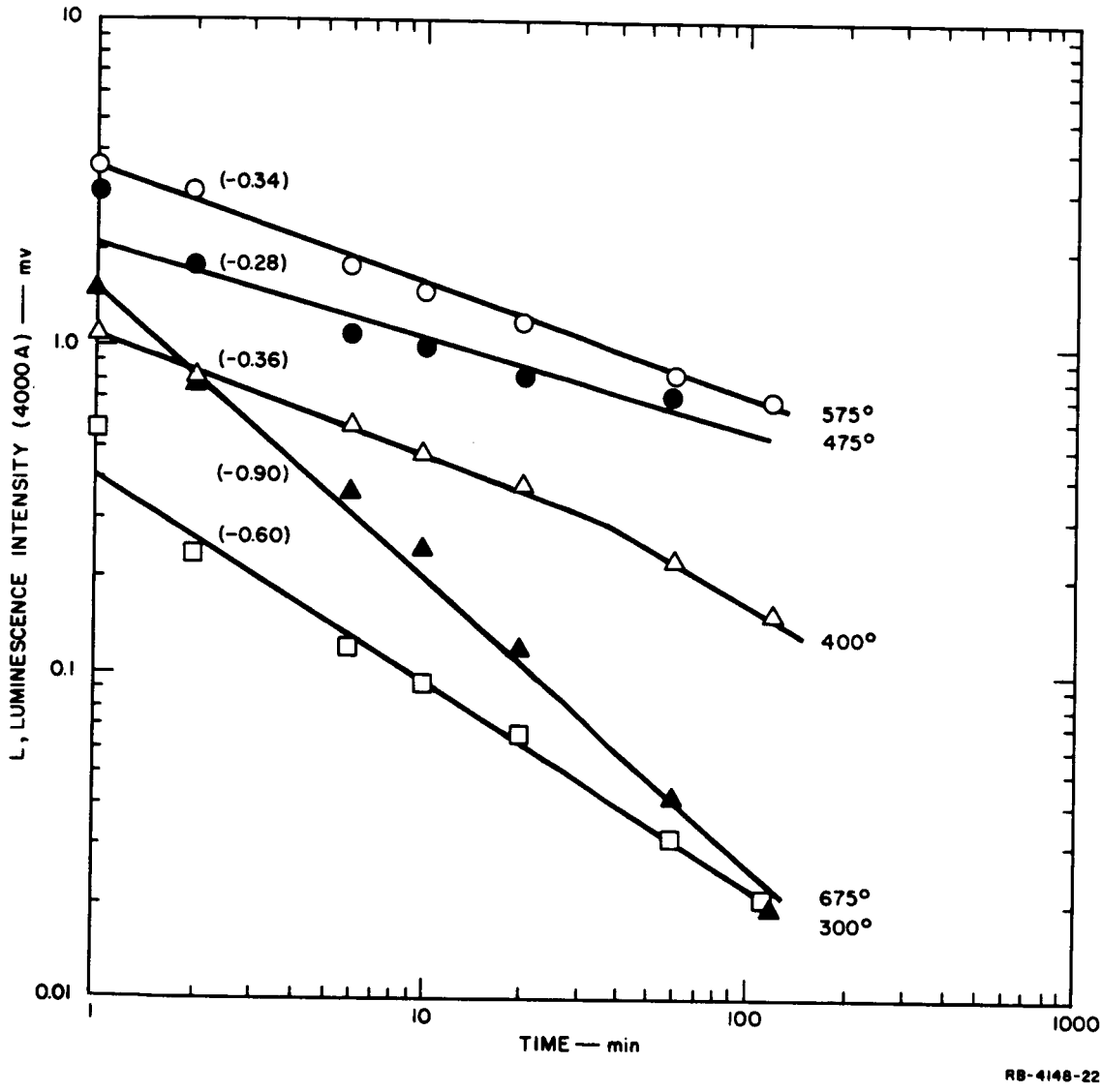

FIG. 9 EFFECT OF TEMPERATURE OF CaO:Sb:Cl(#3) UPON LUMINESCENCE AT 4000A EXCITED BY OXYGEN ATOMS. PRESS. 16μ; DISCHARGE POWER 130 WATTS

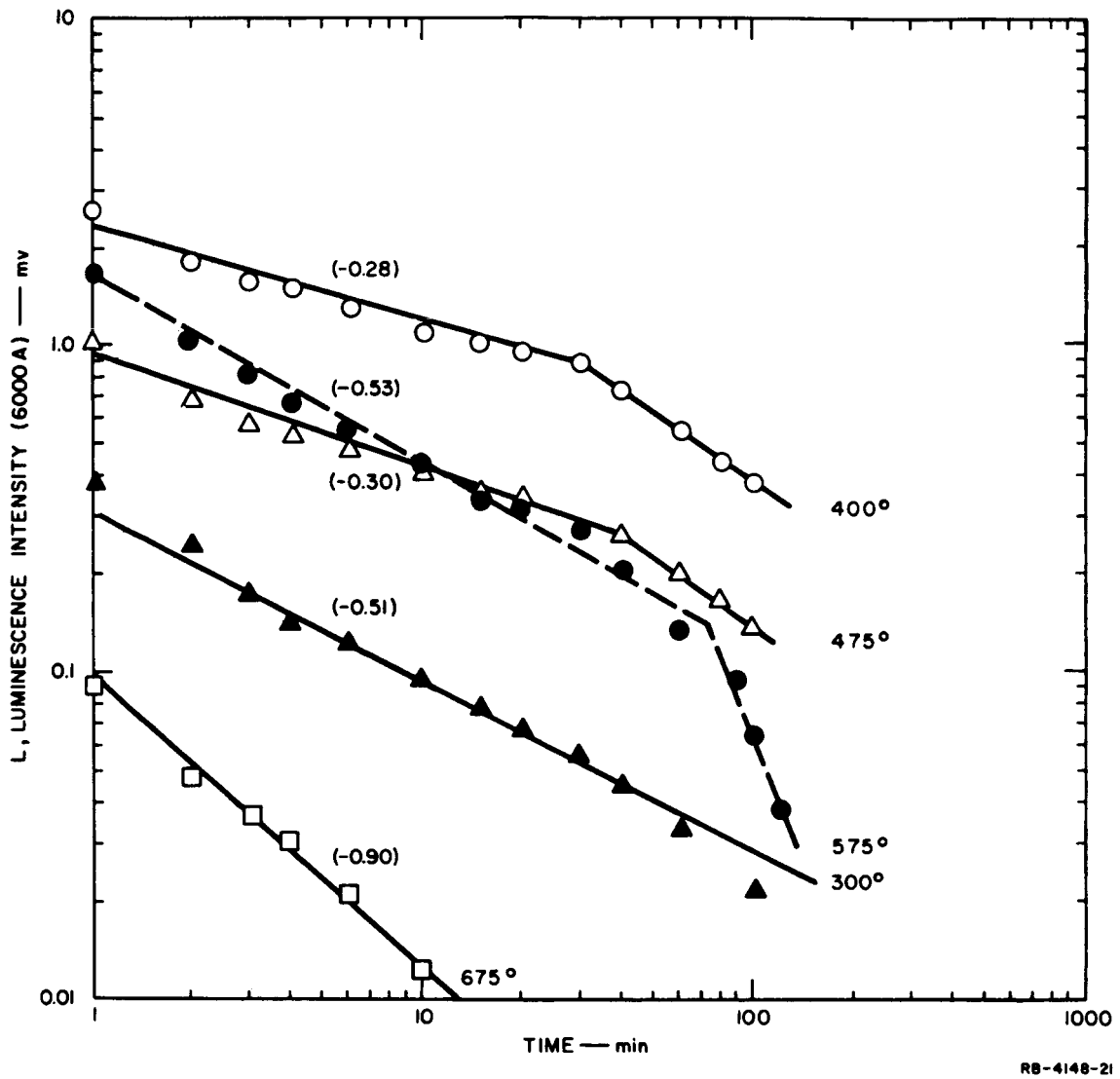

FIG. 10 EFFECT OFTEMPERATURE OF CaO:Mn:Cl(#14) UPON LUMINESCENCE AT 6000A EXCITED BY OXYGEN ATOMS. PRESS. 16μ; DISCHARGE POWER 130 WATTS

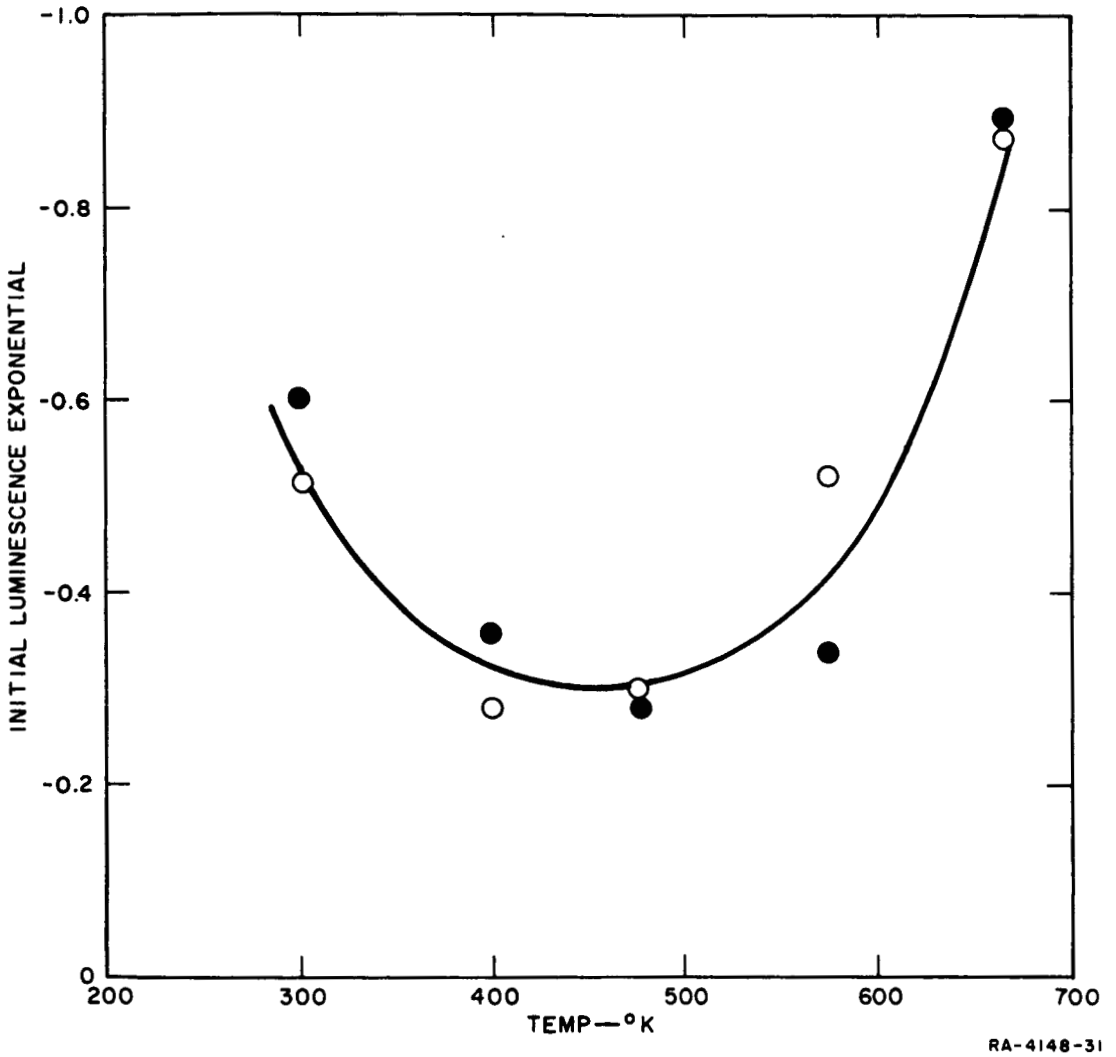

FIG. 11 EFFECT OF TEMPERATURE ON INITIAL LUMINESCENCE EXPONENTIALS OF CaO:Sb:Cl(#3) AT 4000A (SOLID POINTS) AND CaO:Mn:Cl(#14) AT 6000A (OPEN POINTS). PRESS. 16μ; DISCHARGE POWER 130 WATTS

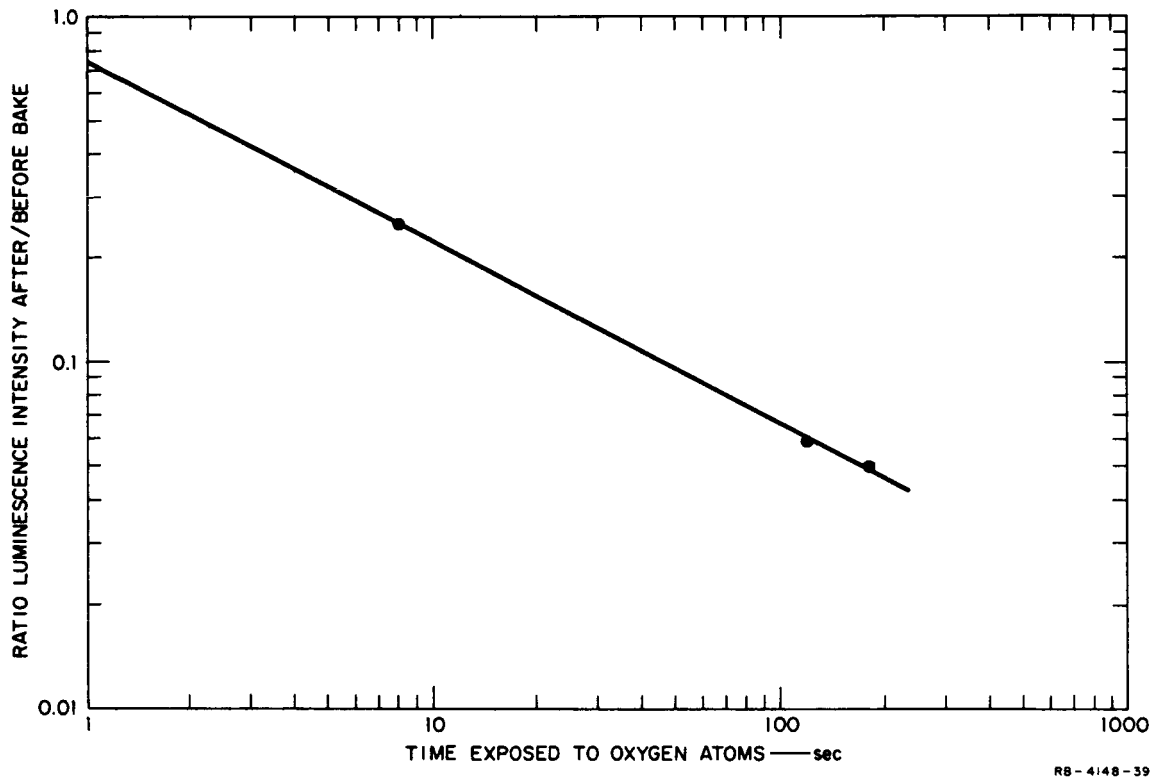

FIG. 12 RATIO OF LUMINESCENCE RESPONSE TO OXYGEN ATOMS AFTER/BEFORE OXYGEN ATOM EXPOSURE OF CaO:Sb:Cl(#3) FOLLOWED BY 10 MIN BAKE AT 800°K IN VACUUM. PRESS. 16μ; DURING ATOM EXPOSURE LUMOPHOR TEMP. 400°K; DISCHARGE POWER 130 WATTS

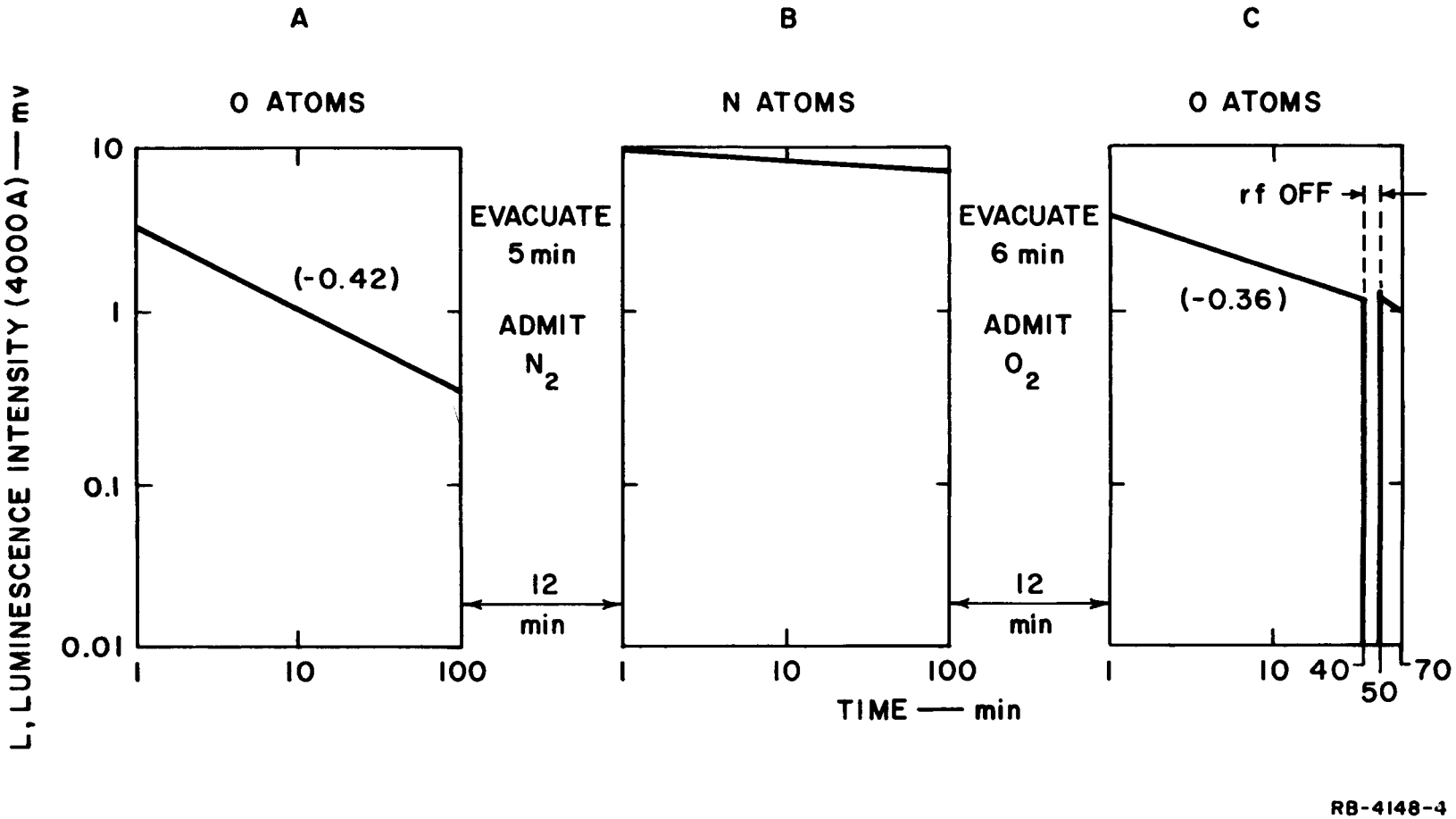

FIG. 13 EFFECT OF EXPOSURE OF A GIVEN SAMPLE OF CaO:Sb:Cl(#3) AT 475°K TO OXYGEN AND NITROGEN ATOMS: (A) INITIAL EXPOSURE TO OXYGEN ATOMS; (B) SUBSEQUENT EXPOSURE TO NITROGEN ATOMS; AND (C) RE-EVALUATION OF RESPONSE TO OXYGEN ATOMS. PRESS. ALL GASES 16μ; DISCHARGE POWER 130 WATTS

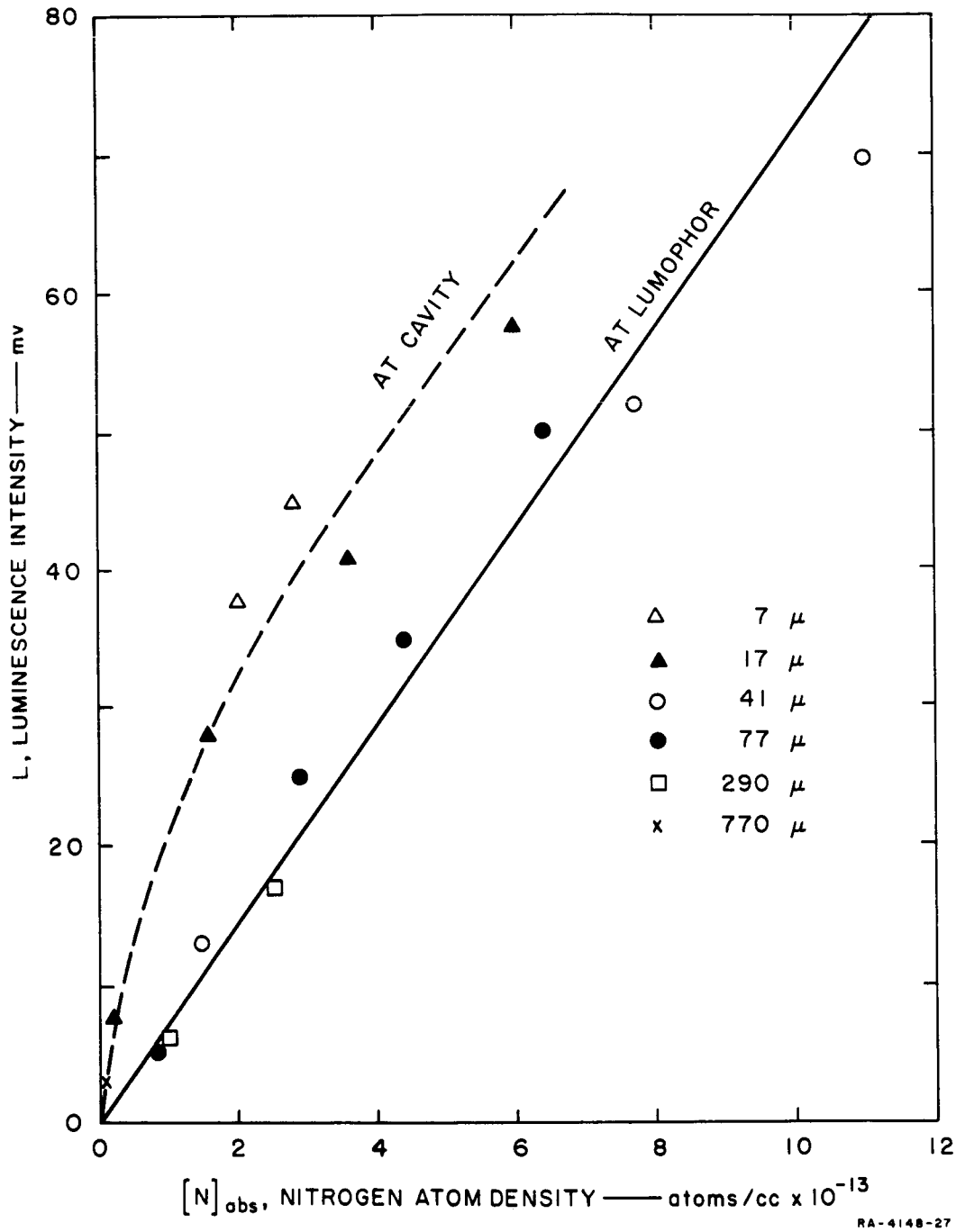

FIG. 14 LUMINESCENCE INTENSITY OF CaO:Sb:Cl(#3) VERSUS NITROGEN ATOM DENSITY AND TOTAL PRESSURE IN RANGE 7 TO 770μ; LUMOPHOR TEMP. 400°K

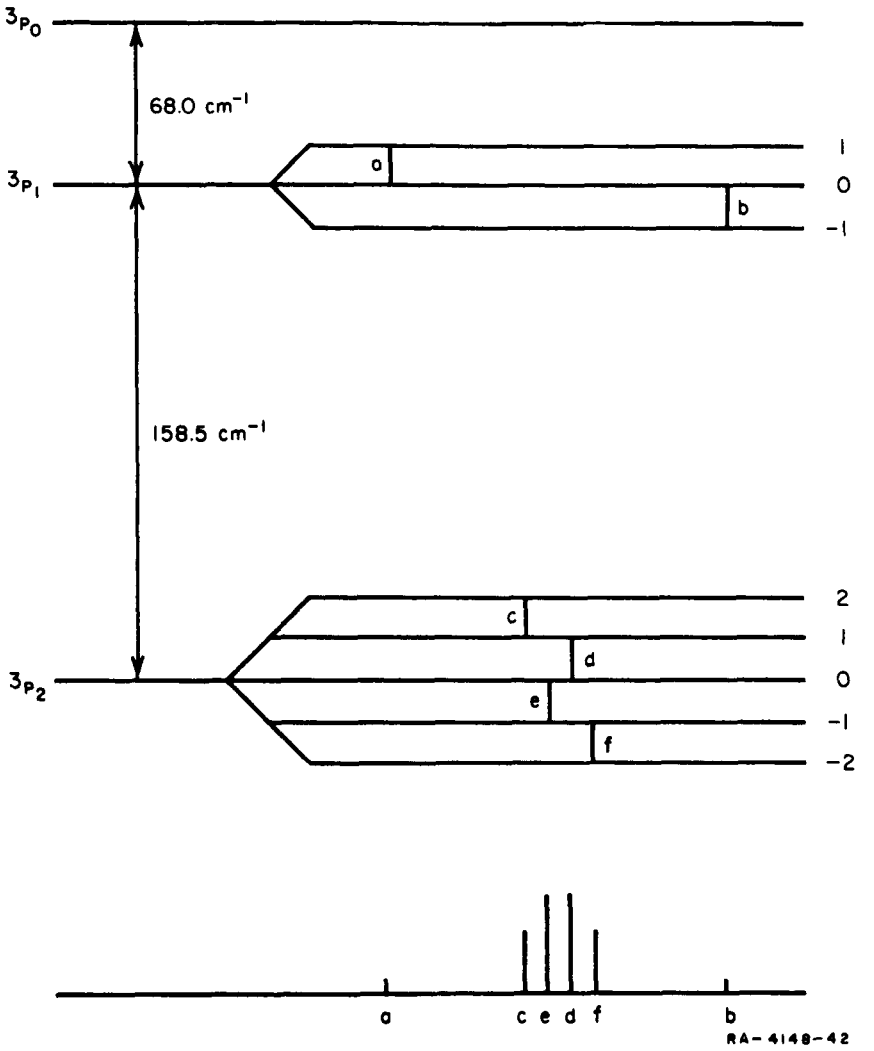

FIG. 15 ENERGY LEVELS AND TRANSITIONS OF ATOMIC OXYGEN IN A MAGNETIC FIELD

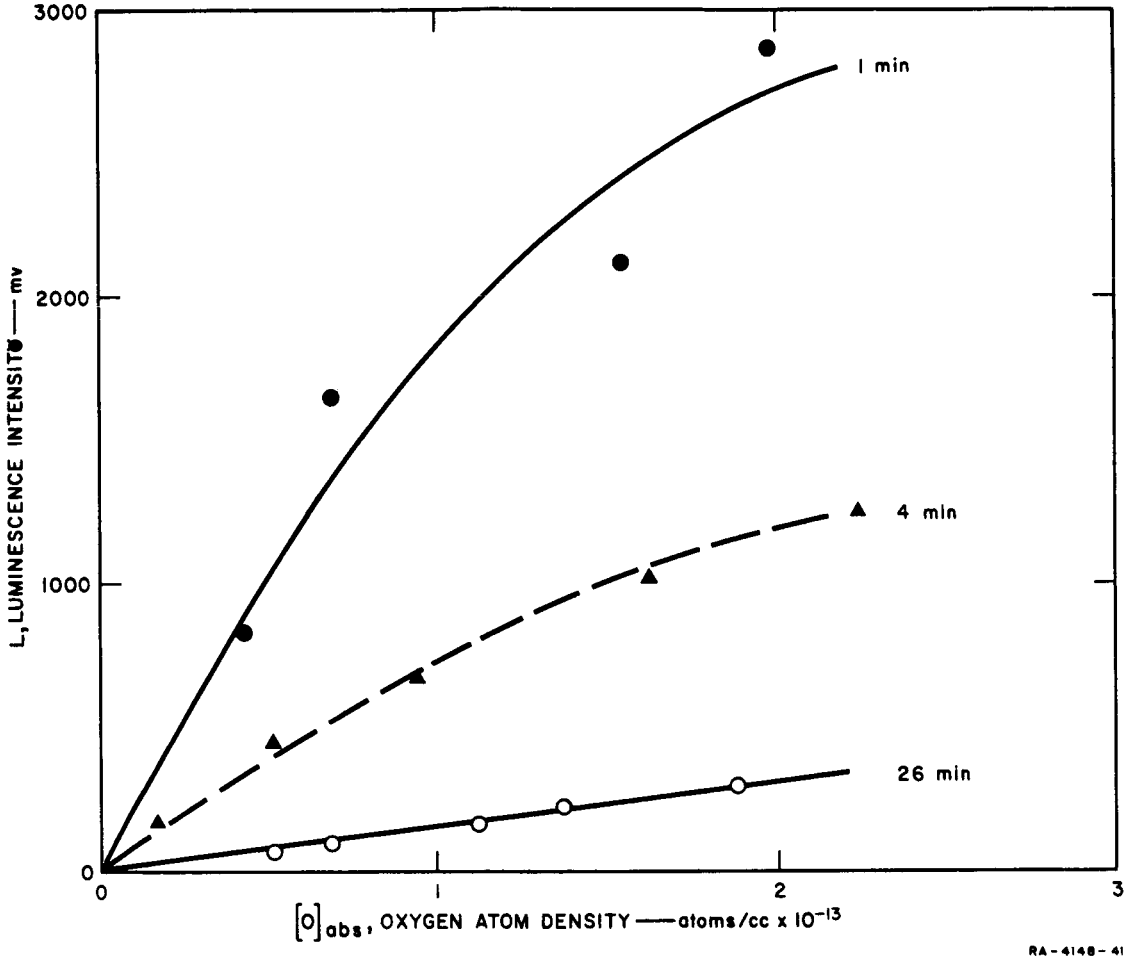

FIG. 16 LUMINESCENCE INTENSITY OF CaO:Sb:Cl(#3) VERSUS OXYGEN ATOM DENSITY AND THE EFFECT OF EXPOSURE TIME TO ATOMIC OXYGEN (DISCHARGE POWER 130 WATTS). ABOUT 1 MIN REQUIRED TO OBTAIN DATA FOR EACH CURVE. PRESS. 16μ; LUMOPHOR TEMP. 400°K

Appendix A

COMPENSATION OF SPECTRAL RESPONSE OF PHOTOOPTICAL SYSTEMS USING A HALL-EFFECT DIODE FUNCTION GENERATOR *

INTRODUCTION

In scientific and engineering investigations it is frequently necessary to correct a direct measurement because of non-linearities of the instrumentation employed. Such a correction can be made automatically by an electronic device known as a function generator. The particular type of diode function generator to be described incorporates a Hall-effect element. This function generator has proven effective in correcting luminescence spectra for the spectral response of a phototube detector and for the spectral transmission of the associated optics, including lens, mirror, and monochromator.

The device may equally well be applied to spectral absorption and transmission measurements. The fully compensated spectrum may be recorded with an X-Y plotter.

Three advantages have led to the choice of a diode function scheme. First, the compensation can be changed quickly and easily to accommodate another optical system -- e.g., a photocell of different spectral response. Secondly, the insertion of gain compensation, $g(\lambda)$, is adjustable (by the user) over a wide range of magnitudes and slopes with respect to wavelength (λ). Finally, the assembly is relatively inexpensive and easily assembled.

---

* This Appendix was originally prepared as a paper to be submitted for publication, and appears here in its original format.

Other alternatives to manual computation of the required response-compensation include nonlinear and multiple-tap potentiometers. The nonlinear potentiometer cannot be adapted from one type of phototube to another, nor -- since it is set by manufacturer -- can the associated transmission properties of the optics be readily compensated. The multiple-tap potentiometer that does not have the latter disadvantage does not allow the compensation gain to be varied at arbitrary wavelengths; furthermore, negative values of the compensation function cannot be easily obtained, as is entirely feasible with a diode function generator.

THE DIODE FUNCTION GENERATOR

A given complex curve is generated by the diode function generator by a combination of a series of piecewise linear curves. Consider a curve of the following general form:

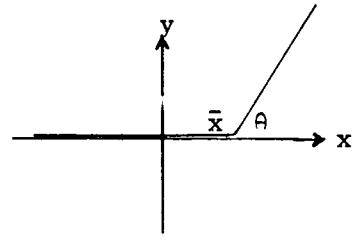

i.e., $y = 0$ for $x \leq \bar{x}$ and $y = x \tan \theta + B$, where B is a constant for $x > \bar{x}$.

Such a piecewise linear curve can be realized experimentally with a simple diode network. Any curve whose maximum rate of change of slope is not excessive can be approximated by a set of such segments. For example, consider the following elementary curve:

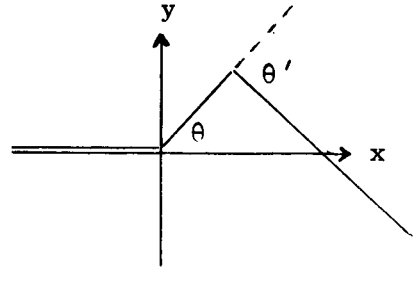

This can be formed by adding two of the above simpler piecewise linear segments -- i.e.,

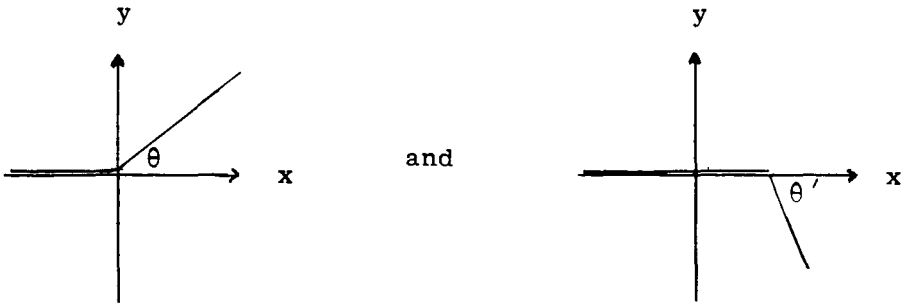

For values of negative x a similar situation holds, using segments of the form:

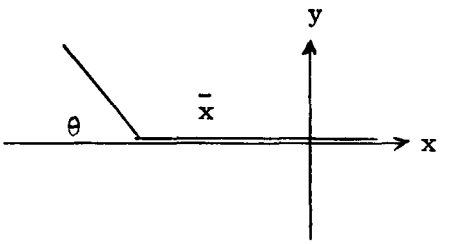

Approximation of a given curve by piecewise segments is accomplished in the function generator, shown schematically in Fig. A-1, by two sets of 12 diode networks, one set for positive x and one set for negative x.

In building up a complex curve in this way, one requires control of two parameters for each segment -- viz., the angle or slope θ, and the distance $\bar{x}$, commonly called the segment break point. In this way a large class of functions can be realized. Thus an input variable λ is processed through a sequence of correctly positioned segments to produce an output function $g(\lambda)$. This is the $g(\lambda)$ shown in Fig. A-2. The detailed method by which $g(\lambda)$ is set up is discussed below.

DESIGN OF HALL-EFFECT DIODE FUNCTION GENERATOR

General

The unit is a combination of a diode function generator and Hall-effect multiplier. There are two inputs to the system. These are:

(1) The uncompensated voltage output $f(\lambda)$ from the photomultiplier (RCA 6217), which is taken here to be the output of a microvolter buffer amplifier.

(2) A voltage $v_x = A + k\lambda$, where A and k are constants and λ is the wavelength of the luminescence sent from the monochromator to the photomultiplier.

If a grating monochromator is used, the angular position of the grating is linearly proportional to wavelength. A helipot geared to the grating rotation provides the voltage v_x as required (Fig. A-3).

The diode function generator input $f(\lambda)$ is modified by some gain function $g(\lambda)$ to correct the nonlinearities of both the optical system and the photomultiplier. This gain function is set in the diode function generator with $A + k\lambda$ as the generator input. The two inputs to the Hall-effect multiplier are therefore $f(\lambda)$ and $g(\lambda)$. The resulting output $f(\lambda)\ g(\lambda)$ is then the required fully compensated photomultiplier signal.

Construction Details

The equipment discussed in this paper was designed for a specific input range $[0 \leq f(\lambda) \leq 1$ volt$]$. Other input ranges may be accommodated by the two input amplifiers I and II (Fig. A-4) because their gains can be varied as required by changing the value of the feedback resistors R1 and R2. At maximum dynamic range the output voltage for the two amplifiers may be 100 volt, and for highest accuracy their gain should be limited to 10.

Amplifiers III and IV are required to process the diode function generator output signals (Points D and E of Fig. A-1). It should be noted that Amplifiers II, III, and IV use chopper stabilizers to keep d.c. drift to a minimum, and Amplifiers II and IV have power boosters so that the Hall-effect multiplier can be adequately driven. The output for the Hall multiplier is of low impedance and can be fed directly to the y input of an X-Y plotter, while the x axis signal is provided by the voltage $(A + k\lambda)$.

The Hall multiplier output $f(\lambda)\ g(\lambda)$ is floating with respect to ground, and should the X-Y plotter not have a floating input (as most of them in fact do) a buffer amplifier would then be required. In the construction, normal precautions against hum pickup and the separation of resistive components from the heating effects of the booster amplifier tubes should be observed.

The amplifiers should be well ventilated and the diode function generator components kept reasonably clear of them. It is recommended that the Hall multiplier be mounted well away from the filament transformer in order to prevent magnetic coupling and hence the induction of 60-cps hum. No trouble with hum was actually experienced, so that the necessity of such spacing has not been confirmed.

The Hall-Effect Element

In a piece of indium antimonide, or similar semiconductor, with a current (I_1) flowing through the material and a magnetic field (B) applied perpendicular to this current, a voltage (v) is induced in a direction mutually perpendicular to both field (B) and current (I_1), where $v = k_1\ B\ I_1$, and k_1 is a property of the material. Thus, if the field is produced by a current I_2 flowing around a soft iron core, $v = k_1\ k_2\ I_1\ I_2$, where k_2 is a constant. This is the situation utilized in the function generator described here. The voltage-time response for changes in I_1 is less than one microsecond. However, I_2 flows in an inductive magnetic circuit and this results in a severe practical limit on the rate of change of B, due to available drive voltage. In the present design, then, the sweep time should be greater than 10 seconds. For this and slower sweeps the response to spectral changes is only limited by the X-Y plotter or the photomultiplier noise filter.

FUNCTION SETUP PROCEDURE

Scaling the Function

Figure A-5 shows the photomultiplier spectral response to a standard light source without $g(\lambda)$ compensation. Also shown is the output after

compensation for spectral response and optical transmission. To obtain a fully compensated response the uncompensated signal $f(\lambda)$ must be multiplied by the reciprocal of the spectral characteristics of the optical system. The present instrument is limited to 100 volt range so that the maximum compensating factor attainable is determined by the minimum value of compensating function (v_{offset}), i.e. $100/v_{offset}$, is the resulting maximum scale correction. This limits the range of wavelength for which a flat response can be obtained. v_{offset} cannot be of excessively low amplitude because any amplifier drift would then result in relatively large changes in $100/v_{offset}$ and hence cause low stability. A value of $v_{offset} \geq 2$ volt for a resulting maximum gain factor of 50 is suggested as a practical limit of the instrument. The chosen value of v_{offset} is set using the y_{offset} and its vernier control (Fig. B-4).

Setting the Break Points and Segment Slopes

The instrument as illustrated has a total of twelve positive and twelve negative segments. The y axis (at x = 0) should be selected so that the compensation function can be realized using all the available segments. If more complex functions are expected, more segments can be incorporated into the instrument by adding to the structure shown in Fig. A-1. A correspondingly higher rated Philbrick power supply would also be necessary.

Before setting up the function, all segments are initially stored at their maximum possible break point so that they do not affect the piecewise linear curve until brought into position as described below.

Consider the typical situation in which the function generator unit is to be used to compensate for the nonlinearities of the spectral properties of the photomultiplier and the associated optics. A tungsten lamp (GE No. 30A-T24/3) which was calibrated by the National Bureau of Standards for spectral radiance is placed in front of the grating.[1] The lamp's

1. R. Stair, R. G. Johnston, and E. W. Halback, J. Res. Natl. Bur. Standards, Vol. 64A, p. 291 (1960).

spectral radiance curve, for a current of 35.0 amps., is drawn on graph paper on the X-Y plotter. The function generator is adjusted, segment by segment, so that the plotter pen matches the radiance curve as the grating is rotated. Knowledge of the distribution of the nonlinearities of the system is therefore not explicitly required.

This curve is matched with piecewise linear segments of the diode function generator using as few x axis break points (diode stages) as are necessary to match the curve. Consider a typical wavelength (λ), and let its position on the x axis be j_+. At j_+ (which first will be at $x = 0$), we bring in one of the stored break points to this position. Now moving to a new proximate position j'_+ at a longer wavelength, the linear gain function $g(\lambda)$ between j_+ and j'_+ is adjusted so that the pen at j'_+ matches the radiance curve. If insufficient slope or (gain) is available, either a shorter segment is necessary or two or more segments are set to break at the j_+th point. Next, a new segment is set to break at $x = j'_+$ and the process is repeated. One can tell when a segment has been brought in far enough, because the output signal will be observed to change at this moment, provided that the segment slope is not exactly zero.

Thus the spectral radiance curve on the X-Y plotter is matched for positive x inputs. The process is again repeated for increasingly negative x values, starting from $x = 0$. Due to possible second-order interactions, for highest accuracy one should retrace the function, making slight corrections to y_{offset} and positive and negative slopes as necessary. The break points are not touched, and they should be indicated along the x axis (Fig. A-2) as a reminder.

Limitations of the Equipment

The initial compensation confirmation is shown by the superimposed X-Y plot over the spectral radiance curves in Fig. A-5. This has remained essentially unchanged over a period of two months.

The highest multiplicative compensation factor consistent with maximal long-term d.c. stability of the unit is about x20 (with preamplifiers I and II limited to x10), although x50 is entirely practical. To compensate for the spectral properties of the optical system described over the wavelength 0.3 to 0.7 μ, a factor of only x17 was needed.

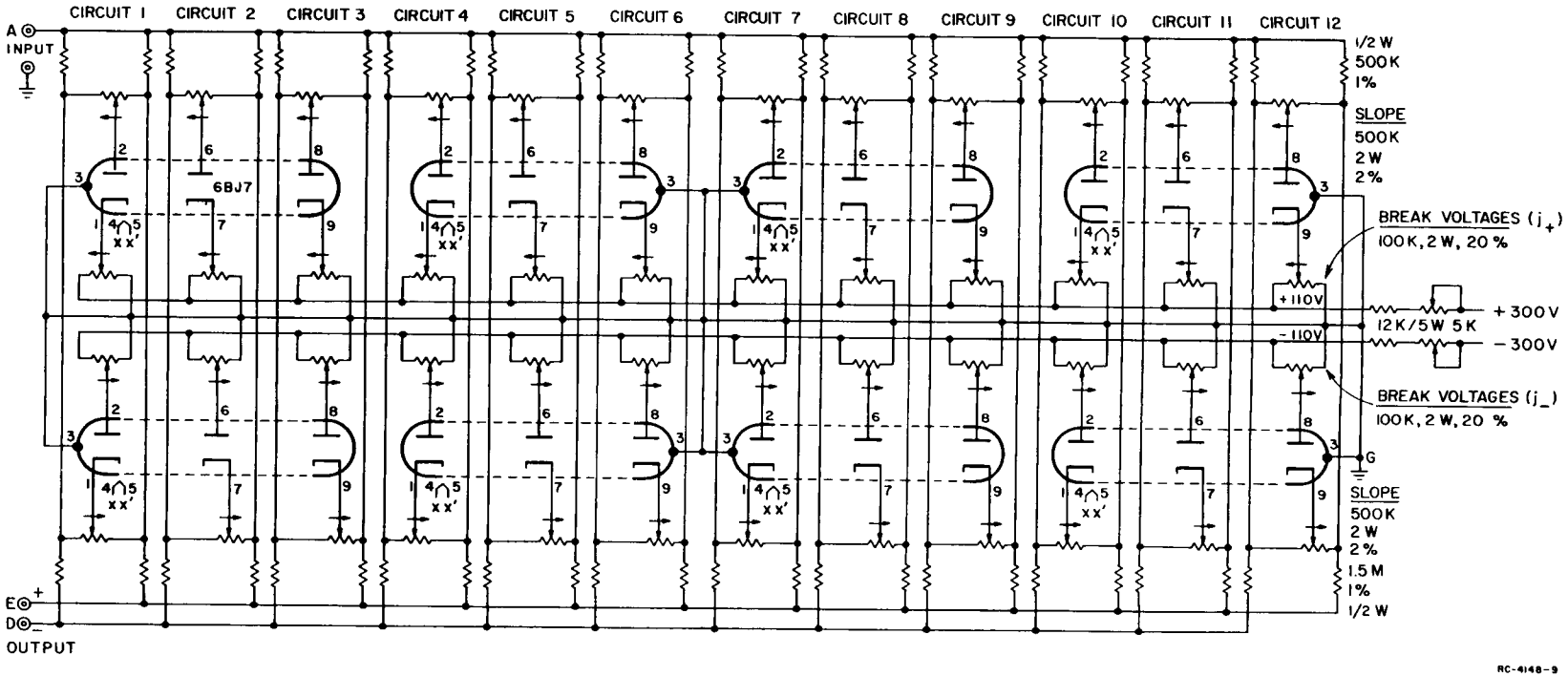

FIG. A-1 DIODE FUNCTION GENERATOR. 12 POSITIVE AND 12 NEGATIVE SEGMENTS ARE SHOWN

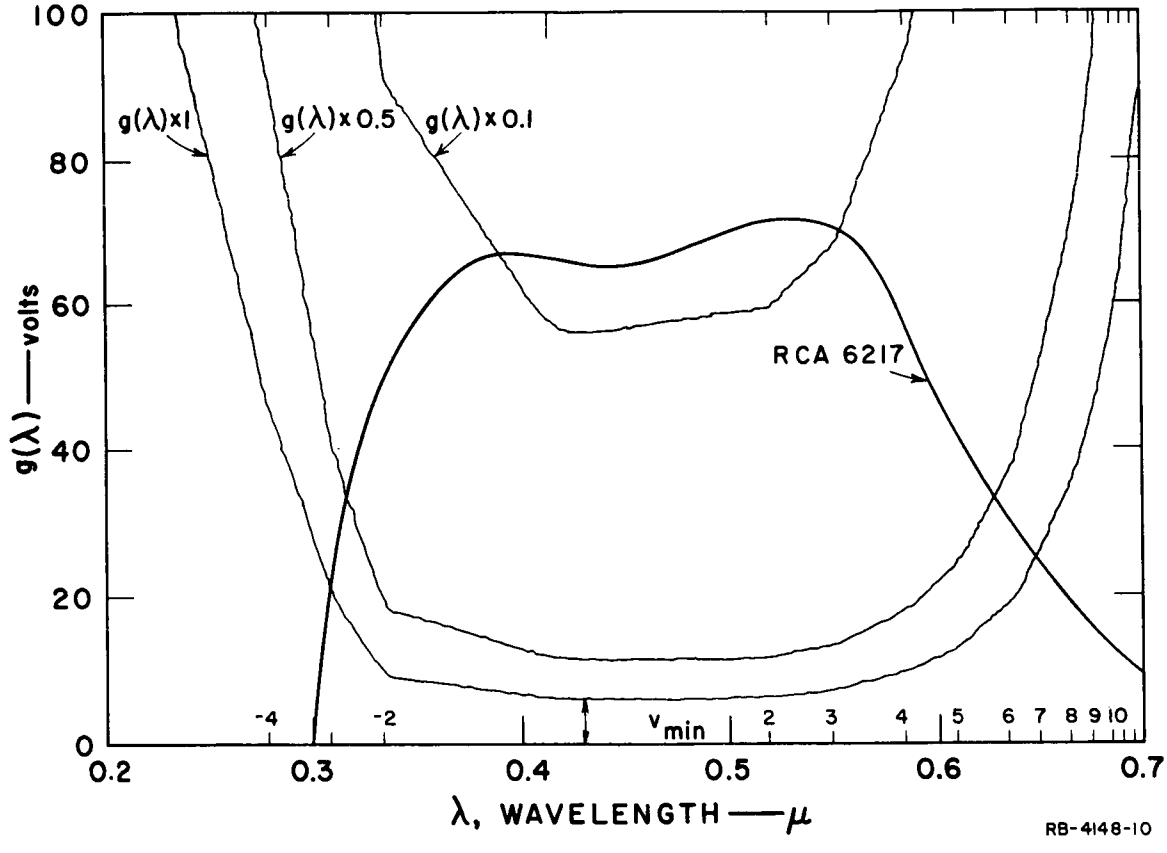

FIG. A-2 TYPICAL OUTPUT FOR DIODE FUNCTION GENERATOR. PHOTOMULTIPLIER (RCA 6217) RESPONSE IS SUPERIMPOSED

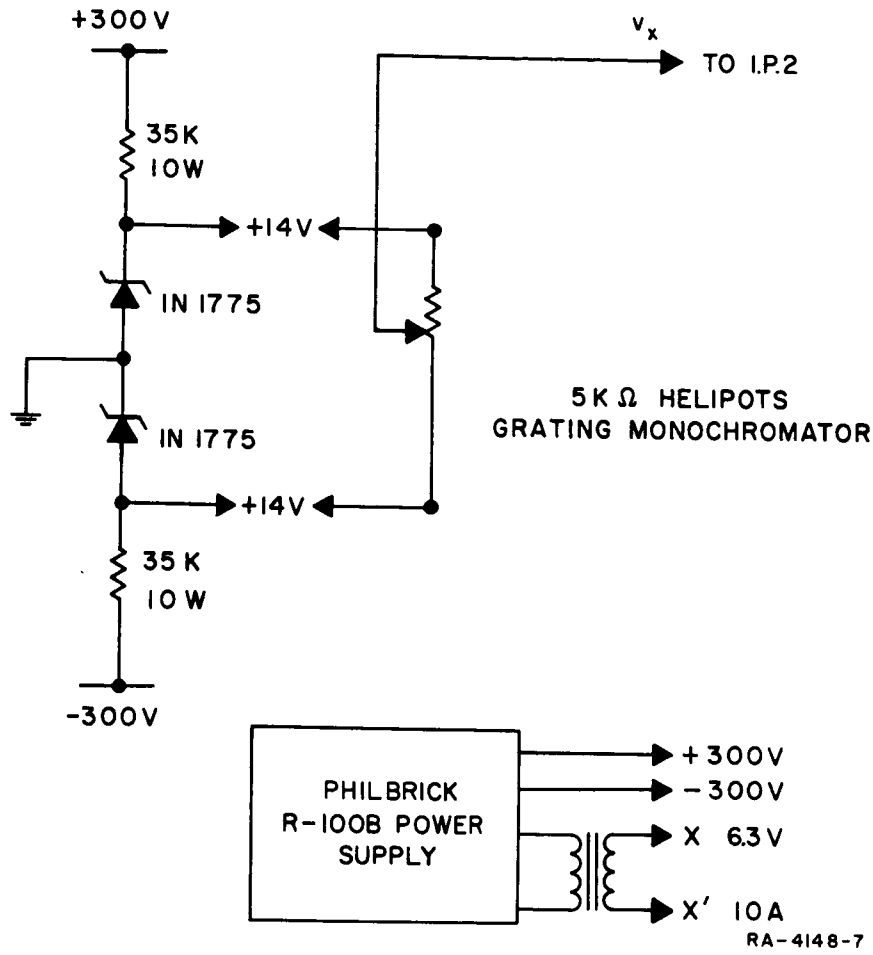

FIG. A-3 UNIT POWER SUPPLIES

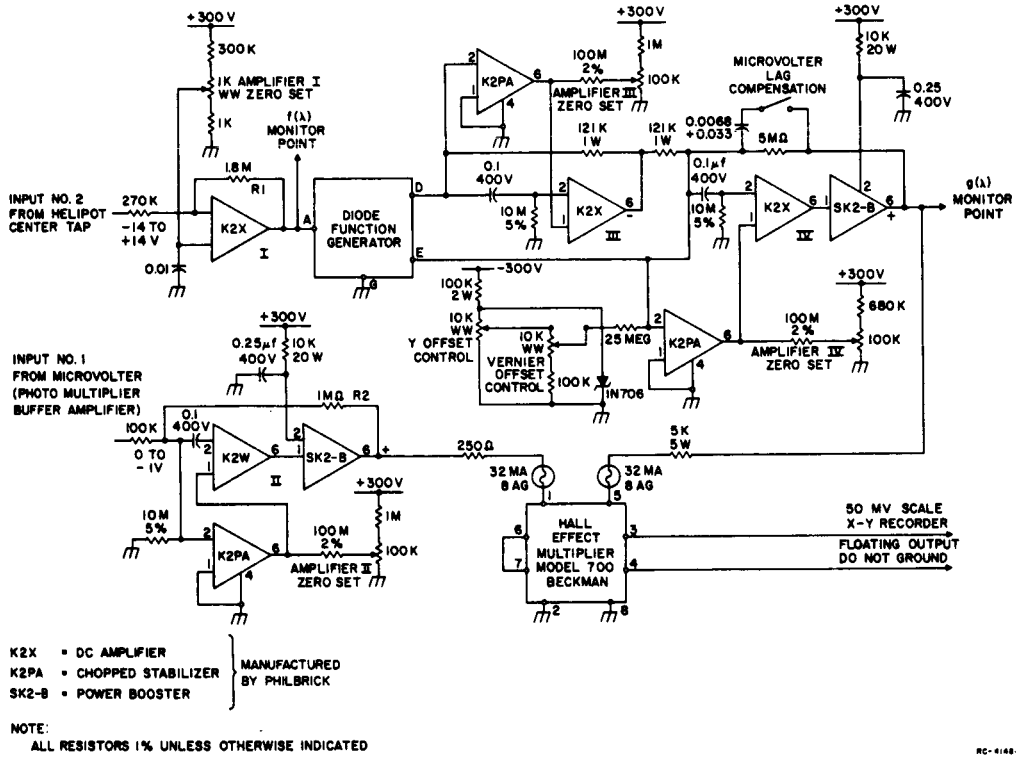

FIG. A-4 MULTIPLIER AND ASSOCIATED CIRCUITRY FOR THE DIODE FUNCTION GENERATOR

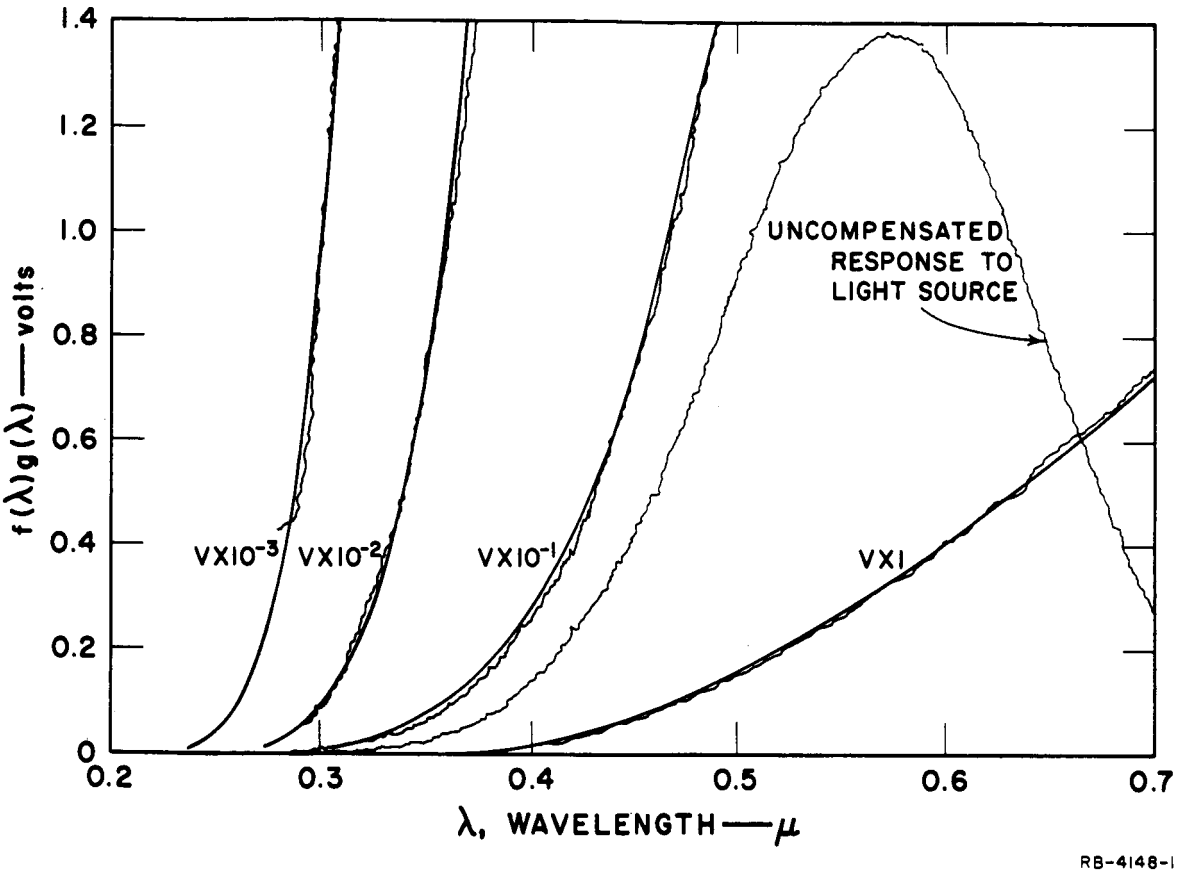

FIG. A-5 X-Y PLOTTED COMPENSATED AND UNCOMPENSATED PHOTOVOLTAGES (JAGGED LINES) OF STANDARD LIGHT SOURCE (35 amps). SOLID SMOOTH LINES ARE THE SPECTRAL RADIANCE OF SOURCE, RELATIVE SCALE CHANGES ARE INDICATED ON EACH CURVE

Appendix B

ABSOLUTE ATOM DENSITY MEASUREMENTS BY ELECTRON SPIN RESONANCE

INTRODUCTION

Electron spin resonance (ESR) spectroscopy was selected to measure absolute densities of nitrogen or oxygen atoms in connection with studies of heterogeneous atom recombination on catalytic surfaces. Molecular oxygen is used to provide a standard of known spin density against which the atom densities may be compared in a system of identical geometry. Tinkham[1,2] has developed the theory of the molecular oxygen ESR spectrum, and Krongelb and Strandberg[3,4] have applied Tinkham's results to obtain absolute oxygen atom densities. Hildebrandt, Barth and Booth[5] have made similar studies with atomic hydrogen, and Wood, Mills and Wise[6] developed the method in detail for atomic hydrogen using first-moments of the ESR derivative lines.

In this discussion we summarize the method of calculating absolute atom densities of nitrogen, hydrogen and oxygen atoms by using molecular oxygen as a standard for spin concentration. The development of the discussion follows principally that of Wood, Mills and Wise,[6] except for considerations of atomic oxygen which follows, with some corrections, Krongelb and Strandberg.[4]

General Mathematical Formulation

Absorption* of microwave energy by a paramagnetic system is described by the imaginary part of the complex susceptibility $\chi = \chi' - i\chi''$ where

---

* One may transform χ'' to χ' through use of Kronig-Kramers transforms,[7] thus the analysis may be used for either absorption or induced emission.

$$\chi'' = \frac{[N_{JM}|(JM|\vec{\mu}_r|J'M')|^2 - N_{J'M'}|(J'M'|\vec{\mu}_r|JM)|^2]}{\hbar} f(\omega-\omega_0) \qquad (1)$$

where $\vec{\mu}_r$ is the magnetic field operator called the dipole moment or permeability vector, J is the total angular momentum, M is the magnetic quantum number, N_{JM} and $N_{J'M'}$ are the populations of the ground and excited spin states respectively. $f(\omega-\omega_0)$ is the absorption resonance line shape function; in this case we follow Krongelb[3] and assume the Bloch shape function. $|(JM|\vec{\mu}_r|J'M')|^2$ is the absolute square of the matrix element for the transitions from the ground state to the excited state and conversely for $|(J'M'|\vec{\mu}_r|JM)|^2$. These quantities give the probability for a transition to occur. Since either transition is equally likely, the following is true

$$|(J'M'|\vec{\mu}_r|JM)|^2 = |(JM|\vec{\mu}_r|J'M')|^2 . \qquad (2)$$

Thus from (1) and (2) we have

$$\chi'' = \frac{(N_{JM}-N_{J'M'})}{\hbar} |(JM|\vec{\mu}_r|J'M')|^2 f(\omega-\omega_0) . \qquad (3)$$

For a system of N atoms whose spin states are in thermal equilibrium we have

$$N_{JM} = \frac{N \exp(-E_{JM}/kT)}{\sum_{JM} \exp(-E_{JM}/kT)} = \frac{N \exp(-E_{JM}/kT)}{Z} \text{ (Ref. 4)} \qquad (4)$$

where Z is the partition sum. For $h\nu_{JM} = E_{JM} \ll kT$ (a general condition for microwave transitions at room temperature) the population difference is

$$N_{JM} - N_{J'M'} = \frac{\hbar\omega}{kT} \frac{N \exp(-E_{JM}/kT)}{Z} . \qquad (5)$$

Hence we may rewrite equation (3) to give

$$\chi'' = \frac{N}{Z}\frac{\omega}{kT} |(JM|\vec{\mu}_r|J'M')|^2 f(\omega-\omega_0) \sum_{JM} \exp(-E_{JM}/kT) . \qquad (6)$$

We must evaluate the terms in χ'' of equation (6) for a one-electron species such as nitrogen or hydrogen atoms.

From Ref. 1

$$|(JM|\vec{\mu}_r|J'M')|^2 = \frac{f_+}{2} |(JM|\mu_+|J'M')|^2 \quad (7)$$

where f_+ is the filling factor. The value of the square of the matrix element is given by[8]

$$|(JM|\mu_+|J'M')|^2 = \tfrac{1}{2} g^2 \beta^2 (J + M)(J - M + 1) . \quad (8)$$

Also by summing over all transitions we obtain

$$\sum_{M=-J+1}^{J} (J + M)(J - M + 1) = \tfrac{2}{3} J (J + 1)(2J + 1) . \quad (9)$$

The partition sum Z is

$$Z = \sum_{JM} (2J + 1) \exp(-E_{JM}/kT) . \quad (10)$$

From Ref. 2

$$f(\omega-\omega_0) = \frac{\hbar}{g\beta} f(H - H_0) . \quad (11)$$

The integrated form of equation (6) is

$$\int \chi'' dH = N(\tfrac{\pi}{2})\left(\frac{\hbar\omega}{g\beta kT}\right) \frac{1}{Z} |(JM|\mu_r|J'M')|^2 \sum_{JM} \exp(-E_{JM}/kT) . \quad (12)$$

It is understood that E_{JM} is the energy of a given transition, $\omega = 2\pi\nu$, where ν is frequency of the absorption resonance; J is the total angular momentum quantum number; g is the spectroscopic splitting factor; k is the Boltzmann constant; T is the absolute temperature; N is the number of atoms; $f(\omega-\omega_0)$ is the shape function for the absorption curve; and β is the Bohr magneton.

In experiments of the type performed here (fixed frequency, variable magnetic field), one can employ the concept of statistical moments for analysis of the recorded output, $d\chi''/dH$. In short, one uses integrated intensity which can easily be taken from the derivative curves. Because the integrated intensity (the first moment of the derivative absorption curve) is used, we should discuss the function of $f(H - H_0)$. Krongelb[3,4] shows that this function is essentially constant and therefore that it integrates to a value of $\pi/2$. Thus we must concern ourselves with summation and integration of the elements of equation (6). Combination of the terms above with equation (6) leads to

$$\int \chi'' dH = \frac{\hbar\omega N}{6kT} \frac{\pi}{2} g\beta J(J + 1) f_+ . \tag{13}$$

The hyperfine splitting of the nucleus plays an important role. Thus if one absorption line is used, the above equation must be corrected (for example, see Ref. 5, p. 2) by $1/(2I + 1)$ where I is the spin of the proton. Thus we have

$$\int \chi'' dH = \frac{\hbar\omega N}{6kT} \frac{\pi}{2} g\beta \frac{J(J + 1)}{(2I + 1)} f_+ \tag{14}$$

or

$$N = \frac{(2I + 1)}{J(J + 1)} \frac{2}{\pi} \frac{6kT}{\hbar\omega\beta g f_+} \cdot \int \chi'' dH . \tag{15}$$

The value of N for a one-electron atom can be computed from equation (15) and from the values of I and J tabulated below.

Atom	Ground Term	I	J	$(2I + 1)/J(J + 1)$
N	$^4S_{3/2}$	1	$^3/_2$	$^{12}/_{15}$
H	$^2S_{1/2}$	$^1/_2$	$^1/_2$	$^8/_3$

The treatment for evaluating the number of oxygen atoms N_O follows that developed by Krongelb and Strandberg,[3,4] with some necessary corrections. They evaluate N_O by summing the terms in equation (12) for the transitions involving the lowest states, $^3P_2$, $^3P_1$, and $^3P_0$. The correct evaluation of the summation term is

$$|(JM|\mu_r|J'M')|^2 \sum \exp(-E_{JM}/kT) = \frac{f_+}{2} g^2\beta^2(49.2) . \qquad (16)$$

(Krongelb[3,4] neglected to carry the g^2 term). The value of the partition sum from equation (10) is given[3] as 6.74. The correct relationship for N_O is then

$$N_O = \frac{1}{3.65} \frac{2}{\pi} \frac{kT}{\hbar\omega\beta g f_+} \int \chi''_O \, dH \qquad (17)$$

and this result for N_O is small by the factor $1/g^2$ than that given by Krongelb (Ref. 4, equation (7)).

Molecular Oxygen

For molecular oxygen the correct integrated form of equation (3) becomes

$$\int \chi''_{O_2} \, dH = N_{O_2} \left(\frac{\pi}{2} \frac{\hbar\omega}{\beta kT}\right) \frac{|(JM|\mu_r|J'M')|^2}{g_{eff}} \frac{\exp(-E_{JM}/kT)}{Z} . \qquad (18)$$

The partition sum Z is approximated by its classical value $3kT/2\beta\hbar$. For molecular oxygen $\beta = 4.31 \times 10^{10}$ cps, so that at 300^0K, $Z = 217$.[3,4]

The matrix element for $\Delta M = \pm 1$ transitions is, as in equation (7),

$$|(JM|\mu_r|J'M')|^2 = \frac{f_+}{2} |(JM|\mu_\pm|J'M')|^2 . \qquad (19)$$

Following Krongelb, for molecular oxygen, $\vec{\mu}$, in Tinkham and Strandberg's notation, is $g_s\beta\vec{S}$. Thus we are concerned with the matrix element

$$|(JM|S_\pm|J'M')|^2 = 4|(JM|S_x|J'M')|^2 . \qquad (20)$$

When Krongelb[3,4] squares the matrix elements of equation (20) he erroneously squares the coefficient 4. Also in substituting equations (19) and (20) into equation (18) he neglects to carry along the g^2.

The correct relationship for N_{O_2} is then

$$N_{O_2} = \left(\frac{2}{\pi}\right) \frac{2kT}{\hbar\omega\beta} \frac{217}{g_{eff} f_{\pm}} \cdot \frac{\int \chi''_{O_2} \, dH}{\left[4 \left|(JM|\mu_x|J'M')\right|^2 \exp(-E_{JM}/kT)\right]} \cdot \quad (21)$$

The bracketed quantity in the denominator may be found in Tinkham and Strandberg (Ref. 2, Table p. 958). We may also use the value $g_{eff} = d\upsilon/dH$ for the particular transition selected. In this paper the transition selected corresponds to the line at 6087.5 gauss (K, J, M are 1, 2, 1 → 2), for which the bracketed quantity is 1.34 and g_{eff} is 1.74.

Computation Formulas

When the same apparatus is used to compare resonance absorption of atom species and molecular oxygen the filling factors are equal, i.e., $f_+ = f_{\pm}$, and the number of species N may be substituted by a density of species $[N]$. The density is conveniently expressed as particles/cc and computed according to the gas law $n/v = P/RT$, which for pressure P in microns (μ) of Hg and a temperature of 300°K becomes

$$[N] = n/v = 3.22 \times 10^{13} P$$

Atom densities may now be determined from the following equations. For nitrogen or hydrogen atoms, divide equation (15) by equation (21) to obtain

$$[\ ]_{abs} = \frac{3(2I + 1)}{217\ J(J + 1)} [O_2] \frac{g_{eff}}{g} \cdot \left[4 \left|(JM|\mu_x|J'M')\right|^2 \exp(-E_{JM}/kT)\right] \frac{\int \chi'' \, dH}{\int \chi''_{O_2} dH} \quad (22)$$

where the notation $[\ ]_{abs}$ is used to signify the absolute particle density determined by the quantum mechanical method. Substituting the appropriate values of I and J, $g = 2.00$, $g_{eff} = 1.74$, and $\left[4 \left|(JM)\right|\mu_x|J'M')\right|^2 \exp(-E_{JM}/kT)]$ = 1.34, the nitrogen atom density $[N]_{abs}$ is

$$[N]_{abs} = 1.29 \times 10^{-2} [O_2] \frac{\int \chi''_N \, dH}{\int \chi''_{O_2} \, dH} . \quad (23)$$

The hydrogen atom density is

$$[H]_{abs} = 4.29 \times 10^{-2} [O_2] \frac{\int \chi''_H \, dH}{\int \chi''_{O_2} \, dH} . \quad (24)$$

The oxygen atom density is calculated by combining equations (17) and (18)

$$[O]_{abs} = 6.30 \times 10^{-4} [O_2] \frac{g_{eff}}{g} [4|(JM|\mu_x|J'M')|^2 \exp(-E_{JM}/kT)] \frac{\int \chi''_O \, dH}{\int \chi''_{O_2} \, dH} , \quad (25)$$

For the molecular oxygen transition specified above, and with g = 1.5 for atomic oxygen

$$[O]_{abs} = 9.81 \times 10^{-4} [O_2] \frac{\int \chi''_O \, dH}{\int \chi''_{O_2} \, dH} . \quad (26)$$

The computation formula for $[O]_{abs}$, equation (25), differs from that reported by Krongelb and Strandberg (Ref. 4, equation (10)). Correction of the errors in the latter, which have been discussed in detail above, result in a computed value of $[O]_{abs}$ smaller by a factor of 3 for the molecular oxygen transition specified in this paper.

In the above equations it is assumed that the first-moments, $\int \chi'' \, dH$, of the relevant resonance lines are measured under identical operating conditions of the ESR spectrometer. In practice it is usually necessary to normalize for the gain G and the magnetic field amplitude for modulation M of the spectrometer; other variables such as microwave attenuation and cryostat isolation are held fixed. The normalized first-moment S is calculated as follows:

$$S = \frac{1}{GM} \int \chi'' \, dH . \quad (27)$$

In this study the value of M is the magnitude (volts) of the 100 kc signal applied to the field modulation coils and measured by a peak-peak voltmeter. The value of the normalized first-moment is independent of the value of M.[9]

First-Moment Definition

For evaluation of the first-moment of the derivative absorption we use the following definition

$$\int_{-\infty}^{\infty} xf'(x)dx \quad = \quad \text{first moment of the derivative } f'(x)$$

Let us integrate this by parts:

$$\int_{-\infty}^{\infty} xf'(x)dx \quad = \quad xf(x)\Big|_{-\infty}^{\infty} - \int_{-\infty}^{\infty} f(x)dx \ . \tag{28}$$

Now if $f(x)$ is of order $1/x^2$, the first quantity on the right-hand side of equation (28) is zero. That is to say, if $f(x)$ is at least Lorentzian in shape, i.e., of order $1/x^2$, then the integrated quantity $xf(x)\Big|_{-\infty}^{\infty}$, disappears leaving

$$\int_{-\infty}^{\infty} xf'(x)dx \quad = \quad \int_{\infty}^{-\infty} f(x)dx \ . \tag{29}$$

Thus for our absorption spectra we may utilize this relationship for evaluation of $\int x''dH$. In short, numerical integration is easily accomplished by recalling the following definition:

$$\int_{-\infty}^{\infty} xf'(x)dx \quad = \quad \lim_{\Delta x \to 0} \sum_{\infty}^{-\infty} xf'(x)\Delta x \tag{30}$$

and thus we may approximate the right-hand side of equation (30) with a high degree of accuracy depending upon how small Δx is chosen.

References

1. M. Tinkham, Theory of the fine structure of the molecular oxygen ground state with an experimental study of its microwave paramagnetic spectrum. Ph.D. thesis, Dept. Physics, Massachusetts Institute of Technology, 1954.

2. M. Tinkham and N. W. P. Strandberg, Phys. Rev. 97, 937 (1955).

3. S. Krongelb, The use of paramagnetic resonance techniques to study atomic oxygen recombinations. Ph.D. thesis, Dept. Physics, Massachusetts Institute of Technology, 1958.

4. S. Krongelb and N. W. P. Strandberg, J. Chem. Phys. 31, 1196 (1959)

5. (a) A. F. Hildebrandt, C. A. Barth, and F. B. Booth, "Atomic Concentration Measurements Using EPR," Progress Report No. 20-371, Jet Propulsion Laboratory, California Institute of Technology, Pasadena, Calif., August 6, 1954.

   (b) C. A. Barth, A. F. Hildebrandt, and M. Patapoff, Disc. Faraday Soc. 33, 162 (1962).

6. B. J. Wood, J. S. Mills, and H. Wise, J. Phys. Chem. 67, 1462 (1963).

7. J. R. MacDonald and M. K. Brachman, Rev. Mod. Phys. 28 (4), 393 (1956).

8. E. V. Condon and G. H. Shortley. The Theory of Atomic Spectra, The University Press, Cambridge, 1959, p. 387.

9. K. Halbach, Phys. Rev. 119, 1230 (1960).

NASA-Langley, 1964